Hacettepe Journal of Mathematics & Statistics

Hacet. J. Math. Stat.
Volume 53 (2) (2024), 556 – 576
DOI : 10.15672/hujms.1269072

Research Article

A novel hybrid ICA-SVM method for detection and identification of shift in multivariate processes

Zümre Özdemir Güler*[1], Mehmet Akif Bakır[2], Filiz Kardiyen[2]

[1] *Aydın Adnan Menderes University, Söke Faculty of Business, Department of Economics, Söke, Aydın, Turkey*

[2] *Gazi University, Faculty of Sciences, Department of Statistics, 06500, Ankara, Turkey*

Abstract

Detecting shifts in the mean vector of a multivariate statistical process control is crucial, and equally important is identifying the source of such a signal. This study introduces a novel approach that combines independent components analysis with support vector machines to address the challenge of multivariate process monitoring. In this hybrid independent components analysis-support vector machines method, statistical metrics I^2 derived from the independent components extracted through independent components analysis from observed data serve as input variables for the support vector machines. The probabilistic outputs generated by the support vector machines model are utilized as monitoring statistics for the proposed control chart, referred to as $I^2-\mathrm{PoC}$. Simulation results validate the effectiveness of the independent components analysis with support vector machines approach in both detecting and identifying shifts in multivariate control processes, whether they follow a normal or non-normal distribution. Furthermore, the results demonstrate the robustness of this method in handling various challenges, including complex relationships between process variables, shifts of varying sizes, and different distribution shapes, when compared to existing approaches in the literature.

Mathematics Subject Classification (2020). 60G35, 62H10, 93C83, 94C12

Keywords. Multivariate statistical process control, shift detection, shift identification, independent component analysis, support vector machines

1. Introduction

Process monitoring plays an important role in achieving high-quality products in industrial processes and ensuring reliable process control [6, 10]. Detecting the transition of a process from a stable state to a non-stable state is a crucial challenge in industrial and service processes. One of the most effective and commonly used tools for this purpose is statistical control charts. The effectiveness of a control chart is determined by how quickly it can detect an out-of-control signal. In some cases, multiple correlated quality variables

*Corresponding Author.
Email addresses: zoguler@adu.edu.tr (Z. Özdemir Güler), mabakir@gazi.edu.tr (M.A. Bakır), fyuva@gazi.edu.tr (F. Kardiyen)
Received: 22.03.2023; Accepted: 22.12.2023

need to be monitored within a single process. When this occurs, monitoring the process using individual control charts while assuming that quality variables are independent may not yield accurate results. Therefore, many studies have been conducted to develop process control tools that consider the joint probability functions of these variables and condense the monitoring statistics into a single indicator.

One of the most well-known Multivariate Statistical Process Control (MSPC) charts is Hotelling's T^2 chart, designed for detecting shifts in a multivariate production process [17]. However, Hotelling's T^2 chart has limitations in detecting small shifts in the process mean vector, as it only considers the last sample [31]. To address this issue, two alternative charts have been developed: the multivariate cumulative sum (MCUSUM) [9] and the multivariate exponentially weighted moving average (MEWMA) [32] control charts. These control charts are sensitive to the size of the shift in the process mean vector. Nevertheless, it is essential for the control chart's performance not to depend on the shift size. In light of Hotelling's T^2 chart's tendency to miss small to moderate shifts in the mean vector, this study also includes an evaluation of the performance of MCUSUM and MEWMA control charts in comparison. Thus, the study demonstrates that the I^2-PoC control charts offer versatility by not being dependent on the shift size, making it valuable tool in various situations.

When dealing with a process that has correlated data, there's a risk of receiving false signals, which can diminish the effectiveness of a control chart. Conversely, detecting and evaluating the presence of multivariate autocorrelation is a challenging task. Fortunately, the literature offers several studies that address the monitoring of autocorrelated multivariate processes [2,4,49].

The use of traditional multivariate Shewhart charts may not be practical for highdimensional systems with collinearities. It is common to employ projection methods, such as Principal Component Analysis (PCA) and Partial Least Squares (PLS), to reduce the dimensionality of the variable space. Several PCA and PLS control charts have been developed for this purpose [7,11,21,25]. However, it's important to note that while PCA is widely used to reduce the dimensionality of problems for understanding process behavior, it can yield incorrect results in nonlinear processes due to the assumption of normality being required [37].

Shewhart-type control charts require that the process follows a normal distribution. There is relatively little literature on alternative multivariate control charts where normality assumption is not guaranteed. One such alternative was proposed by [30]. While the method introduced by [30] has an advantage in simultaneously detecting shifts in both the mean and variance of the process, it is less efficient at detecting signals when the process does follow a normal distribution [38]. Chang and Bai [3] proposed a modified multivariate statistic based on weighted standard deviations specifically designed for skewed distributions.

In the context of MSPC, it is not only essential to detect shifts in a process but also imperative to pinpoint the specific variable(s) responsible for these shifts. As the number of quality variables within a process increases, the investigation into the root cause of a mean parameter shift can incur significant time and operational costs. Consequently, research efforts have been dedicated to developing tools for identifying the sources of these signals. MSPC charts are capable of monitoring multiple variables concurrently. However, they have limitations when it comes to pinpointing the exact source of a shift. The task of identifying the source variable or variables behind a shift remains an open and critical issue that warrants further investigation. The studies by [1] and [16], based on Bonferroni limits, are examples for this purpose. However, they can be applied when dealing with only two quality characteristics, and cannot diagnose the identification number of out-of-control points. Most MSPC charts utilize the quadratic form of the relevant test statistic. Once a shift in the mean vector of the control chart is detected, a distinct procedure is employed to identify the vector component(s) that constitute it. These procedures are typically grounded in the decomposition techniques outlined in references [15,38–40], and include stepwise procedures akin to those detailed by [45].

In this context, Independent Components Analysis (ICA) is a method that addresses the problem of blind source separation by separating the multivariate data derived from the process into its Independent Components (ICs). ICA calculations are more intricate compared to PCA and PLS, but they offer an additional benefit thanks to the independence between ICs. Latent variables may exist in processes where a dependency exists between monitored variables. These latent variables represent combinations of independent variables that cannot be directly measured. ICA is a method used to extract these latent variables from the observed variables. Due to this advantageous feature of ICA, it has found numerous successful applications in the literature [13,23,26,27,29,51].

Lee et al. [29] introduced three process monitoring statistics, I^2 and I_e^2 , and the Square of Prediction Error (SPE), to detect shifts in the process using ICA. The choice of these monitoring statistics depends on the rank of the ICs. However, it's important to note that there is no standard method for ranking components in ICA. While some methods exist in the literature to rank components obtained through ICA, these methods rely solely on mean square error, making them challenging to apply as the number of variables increases.

In addition to this, Lee et al. [27] proposed modifications to the ICA algorithm to address its limitations, such as the lack of prior knowledge about the number of extracted components and the absence of a standard ranking method for these components. Yoo et al. [50] developed a multiway ICA-based monitoring scheme for process monitoring, while Lu et al. [36] applied ICA to integrate process control in engineering. On a different note, Hsu et al. [19] devised a process monitoring scheme based on ICA and made adjustments to handle outlier observations.

Since most traditional MSPC tools rely on the assumption of normality, various process control tools have been developed based on machine learning algorithms. Machine learning algorithms, initially designed primarily for classification tasks, have been adapted for unsupervised one-class classification to distinguish in-control and out-of-control process data. Among these algorithms, Support Vector Machine (SVM) stands out as a widely used supervised learning technique capable of efficiently handling high-dimensional data from non-normal distributions [14]. The SVM approach has found numerous successful applications, particularly in classification problems, and it doesn't require assumptions about the data distribution.

One notable application is the utilization of SVMs in multivariate control charts based on kernel distance, as proposed by [46]. The study has demonstrated that kernel distance SVM outperforms traditional monitoring methods, especially when dealing with quality characteristics that are not multivariate normally distributed.

In their study, Chongfuangprinya et al. [8] employed a combination of the SVM algorithm and the bootstrap method for MSPC. They utilized SVM classification probabilities as monitoring statistics and derived control limits for this chart, referred to as SVM-PoC, by estimating percentiles of the PoC statistics through the bootstrap method. Their research demonstrated that the SVM-PoC chart outperforms other MSPC charts, particularly in non-normal situations. Furthermore, they developed an Exponential Weighted Moving Average (EWMA) version of the SVM-PoC chart to enhance its sensitivity to small process shifts. While their work successfully addressed the challenge of detecting shifts in the process using SVM classification, it should be noted that they did not present a solution for identifying the source of the signal.

Model-based MSPC methods were developed by leveraging the physical and mathematical structures of a process and have found success in process monitoring. However, these methods may encounter challenges when applied to dynamic and nonlinear processes with varying conditions. This is primarily due to their reliance on assumptions of normality and stationarity. It's important to note that most of the other methods mentioned earlier are also model-based and share this normality assumption for the joint distribution of variables. In situations where the joint distribution is non-normal or unknown, the use of data-driven methods can offer advantages. To enhance the effectiveness of process monitoring tools, its often beneficial to integrate data-driven techniques with model-based approaches. This integration should be done while carefully considering the pros and cons of each approach.

To develop an approach based on SVM when working with high-dimensional data, first and foremost, it is necessary to employ feature extraction methods. To achieve this objective, several approaches have been proposed that involve the integration of ICA and SVM. For instance, Hsu et al. [18] introduced a novel method that combines ICA and SVM. Performance evaluations have shown that ICA-SVM outperforms PCA-SVM. This is attributed to ICA's consideration of higher-order statistics. From this perspective, one can conclude that ICA plays a crucial role in providing more valuable information for SVM to detect process shifts. Another study by Shao et al. [43] suggests a hybrid method that combines ICA and SVM to identify the quality variables responsible for signal variations in a multivariate process.

The method described in the present study, called as the I^2-PoC control chart, is based on the integration of ICA and SVM. It distinguishes itself from similar methods like those presented by [18] and [43], which solely detect signals, by also identifying the source of the signal. However, both Hsu et al. [18] and Shao et al. [43] have certain limitations. They do not account for the correlation structure between variables and do not consider non-normal processes. The I^2-PoC control chart is formed by combining ICA, which extracts features while preserving dependency structures, and SVM, a classifier that does not rely on normality assumptions. Consequently, this approach ensures that the process distribution remains unaffected by the correlation structure between variables, eliminates the need for assuming normality in the process distribution, and is independent of the shift size. Therefore, it can be concluded that the proposed method offers greater flexibility and functionality compared to alternative approaches.

The remainder of this study is structured as follows: Section 2 introduces the theoretical frameworks of ICA and SVM. In Section 3, we delve into the specifics of the proposed method. Chapter 4 provides a detailed account of the simulation study conducted to assess the performance of our proposed approach. Section 5 is dedicated to interpreting the findings derived from the simulation studies. Lastly, Section 6 hosts discussions concerning the results.

2. Preliminaries

In this section, the theoretical structure of ICA and SVM methods is explained.

2.1. Independent component analysis

ICA [12,22] is a signal processing technique used to transform observed multivariate data into components that are statistically independent and expressed as linear combinations of sources. In other words, ICA is a type of Blind Signal Separation (BSS) method used to separate data into essential sources of information. ICA was originally developed to deal with problems similar to the cocktail party problem, but later this method has been successfully applied in various fields such as image processing, face recognition, and time series estimation [5,33–35]. All of the applications can be formulated in a common mathematical framework for the use of ICA.

In the ICA, it is assumed that p measured variables $\mathbf{X} = [\mathbf{x}(1), \mathbf{x}(2), \ldots, \mathbf{x}(n)] \in R^{p\times n}$ can be expressed as linear combinations of $d(p \leq d)$ unknown ICs $\mathbf{S} = [\mathbf{s}(1), \mathbf{s}(2), \ldots, \mathbf{s}(n)] \in$

$R^{d\times n}$. The relationship between ICs and measurement variables can be written as in Equation 2.1

$$\mathbf{X}=\mathbf{A}\mathbf{S}+\mathbf{E} \tag{2.1}$$

where $\mathbf{A}=[\mathbf{a}_1,\mathbf{a}_2,\ldots,\mathbf{a}_d]\in R^{p\times d}$ is the mixing matrix, $\mathbf{E}\in R^{p\times d}$ is the residual matrix and n is the sample size. The main problem of ICA is to predict both the original components matrix $\mathbf{S}$ and the mixing matrix $\mathbf{A}$ from the observed measurement data matrix $\mathbf{X}$ without any knowledge of the $\mathbf{S}$ or $\mathbf{A}$ matrices. Therefore, the purpose of ICA is to estimate the separation matrix $\mathbf{W}\in R^{d\times p}$. Thus, the $(\hat{\mathbf{S}})$ elements of the estimated sources are as independent of each other as possible. It can be obtained with the formula in Equation 2.2:

$$\hat{\mathbf{S}}=\mathbf{W}\mathbf{X} \tag{2.2}$$

where $\hat{\mathbf{S}}=[\hat{\mathbf{s}}(1),\hat{\mathbf{s}}(2),\ldots,\hat{\mathbf{s}}(n)]\in R^{d\times n}$ is the estimated source matrix and each $\hat{\mathbf{s}}_i, i=1,2,\ldots,d$ vectors are independent from the others.

The ICA modeling is performed in the framework of an optimization problem. This is achieved by defining a measure for the independence of ICs as the primal objective function. Various optimization techniques are then applied to solve the seperation matrix W. Statistically independent ICs have non-Gaussian distributions, and this non-Gaussian state can be measured by negentropy [20]:

$$J(y)=H\left(y_{\text{gauss}}\right)-H(y) \tag{2.3}$$

where y_{gauss} is a Gaussian random variable with the same variance as y. The differential entropy H of the random variable y with the probability density function $f(y)$ is obtained with $H(y)=-\int f(y)\log f(y)dy$.Negentropy is nonnegative and measures the degree of departure from Gaussianity. To predict negentropy effectively, Hyvärinen and Oja [20] developed a simpler approach as in Equation 2.4:

$$J(y)\approx[E\{G(y)\}-E\{G(v)\}]^2 \tag{2.4}$$

where the mean and the variance of y are assumed to be zero and one, respectively. v is the Gaussian variable with zero mean and unit variance, and G is any non-quadratic function and in this study it is accepted as $G_1(u)=\frac{1}{a_1}\log\cosh(a_1u)$ which was used in [28] $(1\leq a_1\leq 2)$

There are various algorithms developed to eliminate computational complexities and accelerate operations in achieving ICs. In this study, the FastICA algorithm proposed by [20] was used to estimate the seperation matrix W. There are two preprocessing steps before the ICA modeling: centering and whitening. Firstly, the input matrix $\mathbf{X}$ is centered by $\mathbf{x}_i\leftarrow(\mathbf{x}_i-E(\mathbf{x}_i))$. The centered input matrix $\mathbf{X}$ then passed through the whitening matrix $\mathbf{Q}$ to extract the quadratic statistic of the input matrix. Whitening transformation $\mathbf{A}$ that removes all cross-correlation between random variables is given by $\mathbf{z}(k)=\mathbf{Q}\mathbf{x}(k)=\mathbf{Q}\mathbf{A}\mathbf{s}(k)=\mathbf{B}\mathbf{s}(k)$ where $\mathbf{Q}=\mathbf{\Lambda}^{1/2}\mathbf{U}^T,\mathbf{Q}\in R^{p\times p}$ is the whitening matrix and it can be calculated with the eigen-decomposition of the covariance matrix $\mathbf{R}_\mathbf{x}=E\left(\mathbf{x}(k)\mathbf{x}^T(k)\right)=\mathbf{U}\mathbf{\Lambda}\mathbf{U}^T$. $\mathbf{B}$ is an orthogonal matrix and is obtained by the $E\left\{\mathbf{z}(k)\mathbf{z}^T(k)\right\}=\mathbf{B}E\left\{\mathbf{s}(k)\mathbf{s}^T(k)\right\}\mathbf{B}^T=\mathbf{B}\mathbf{B}^T=I$.

In this paper, the I^2 value to be used as an input variable to the SVM model has been determined as a single value obtained from separation matrix $\mathbf{W}$ differently from [29]. Thus, the I^2 monitoring statistic for sample k, which is the sum of the squared ICs, is calculated as in Equation 2.5:

$$I^2(k)=\hat{\mathbf{s}}(k)^T\hat{\mathbf{s}}(k) \tag{2.5}$$

The control limit of the I^2 control chart based on ICA were determined by the bootstrap method used kernel density functions since there is no distribution information of ICs. If the monitoring statistics in the I^2 control chart exceed the control limit, it is decided that the process is out of control. This control chart is one-sided since process control is provided by one control limit.

2.2. Support vector machine

SVM is a powerful machine learning method based on statistical learning theory, originally proposed by [48]. It is also known as Vapnik-Chervonenkis theory. SVM was initially designed to optimally separate linearly separable data and was later improved to classify multidimensional and nonlinearly separated data. It is fundamentally based on the principle of determining the hyperplane that can most accurately separate the classes from each other [47].

The training data set consisting of N observations such as $(\mathbf{x}_1, y_1), \ldots, (\mathbf{x}_N, y_N)$ can be represented as $D = \{(\mathbf{x}_i, y_i), i = 1, \ldots, N\}$, with $\mathbf{x} \in R^p$ being any sample in p-dimensional space (input variable) and $y_i \in \{-1, +1\}$ being the class labels to which output variables belong. In order to linearly separate the training data set D containing N independent and identically distributed (iid) samples, the equation of the line of the optimum hyperplane is $\mathbf{wx} + b = 0$. Here $\mathbf{w} \in R^p$ is the optimal weight vector and b is the threshold value. The distance between the hyperplanes separating the classes with maximal margin width $2/\|\mathbf{w}\|^2$, and all the points under the boundary are called support vector. Therefore, the optimal hyperplane can be found by solving the following quadratic optimization problem for a linearly separable case [24]:

$$\begin{aligned} &\operatorname{Min} \frac{1}{2}\|\mathbf{w}\|^2 \\ &y_i(\mathbf{wx} + b) \geq 1, \quad i = 1, \ldots, N \end{aligned} \tag{2.6}$$

This optimization problem can be solved in primal space according to the parameters $\mathbf{w}$ and b. However, solving the dual form of the problem would be a more rational way as it would give the same result as the primal model and depend only on the Lagrange multiplier α_i. Therefore, the primal model in Equation 2.6 is converted to the following dual model:

$$\begin{aligned} &\operatorname{Max} L(\alpha) = \sum_{i=1}^{N} \alpha_i - \frac{1}{2} \sum_{i=1}^{N} \sum_{j=1}^{N} y_i y_j \alpha_i \alpha_j \langle \mathbf{x}_i, \mathbf{x}_j \rangle \\ &\alpha_i \geq 0, i = 1, \ldots, N \\ &\sum_{i=1}^{N} \alpha_i y_i = 0 \end{aligned} \tag{2.7}$$

In most real-life problems, the data may not be linearly separated. In the non-linearly separable case, SVM transforms the original input space into a high-dimensional feature space. This facilitates the identification of an optimal linear separation hyperplane using kernel methods for problems in non-linearly separable input space. There are various options for the kernel function, the most commonly used kernel function is the RBF kernel function, which is defined as $K(\mathbf{x}_i, \mathbf{x}_j) = \exp\left(-\gamma \|\mathbf{x}_i - \mathbf{x}_j\|^2\right)$ where γ is a kernel parameter [44].

The original SVM was designed for binary classifications. In this study, a new process monitoring procedure has been developed with the probability of classification (PoC) of the SVM model. To derive the PoC from the SVM model, Platt [42] used a parametric sigmoid function model with two parameters A and B. After determining the A and B parameters, the PoC of a test dataset $\mathbf{z}_i$ can be obtained from Equation 2.8:

$$\mathrm{PoC}_i = \frac{1}{1 + \exp\left(Af(\mathbf{z}_i) + B\right)} \tag{2.8}$$

Details regarding the calculation of the PoC in SVM can be found in Platt's work [42]. Chongfuangprinya et al. [8] established a threshold value of 0.50 and demonstrated successful classification using SVM-PoC values in both normal and non-normal scenarios.

In the present study, we propose PoC control chart inspired by Chongfuangprinya et al.s research [8]. However, unlike the aforementioned study, we employ misclassification probabilities as process monitoring statistics to simplify the calculation process. When the probability distribution of the monitoring statistic is known, control limit for the control chart can typically be determined based on a specified probability distribution, with a user specified value (eg. Type 1 error rate). Since the distribution of monitoring statistics is unknown in the PoC control chart, we determine the control limit using a bootstrap technique involving kernel density functions. This one-sided control chart focuses on shifts in one direction, specifically targeting upward shifts in the process.

3. Proposed method

This section introduces a hybrid procedure that combines the feature extraction method ICA with the classification method SVM. The proposed hybrid approach is motivated by the idea that the information embedded in the monitoring statistics, used for detecting shifts in the process, can also be valuable in identifying the source of the variable(s) causing the shift. The SVM provides valuable information when utilizing the output of higher-order ICA statistics to detect out-of-control situations in the process. In this context, we treat the process variables and ICA statistics as an input vector for the SVM. The PoCs derived from the SVM are subsequently employed in the computation of the process monitoring statistic $(I^2 - \mathrm{PoC})$.

The hybrid ICA-SVM method is carried out in two stages. In the first stage, the data is used for training to create a classification model. In the second stage, the trained model is put to the test. The initial step involves generating reference information for the hybrid ICA-SVM approach, which considers two states: the normal operating condition (NOC), representing when the process is in control, and the fault operating condition (FOC), representing when the process is out of control [18]. To construct the NOC training dataset, the first task is to scale the NOC dataset. The scaling involves centralisation and whitening of the NOC (in-control process) dataset $\mathbf{x}_{\text{normal}}$.

These changes help to make the text flow more smoothly and clarify the order of actions in the two stages of the method. Next, the FastICA algorithm is executed using the scaled dataset, assuming that the number of process variables equals the number of ICs. FastICA produces both the decomposition matrix and the corresponding orthogonal decomposition matrix.

The relationship between $\mathbf{W}_{\text{normal}}$ and $\mathbf{B}_{\text{normal}}$ is established as

$$\mathbf{B}_{\text{normal}} = \left(\mathbf{W}_{\text{normal}}\mathbf{Q}^{-1}\right)^T . \tag{3.1}$$

Therefore, the estimation of reconstructed signals can be calculated using the formula:

$$\hat{\mathbf{s}}_{\text{normal}} = \mathbf{B}_{\text{normal}}^T \mathbf{z}_{\text{normal}} . \tag{3.2}$$

The monitoring statistics under NOC for the sample t is given in Equation 3.3:

$$I_{\text{normal}}^2(t) = \hat{\mathbf{s}}_{\text{normal}}^T(t)\hat{\mathbf{s}}_{\text{normal}}(t) \tag{3.3}$$

The similar procedure is followed for FOC dataset. The ICs under FOC can be calculated as follows:

$$\hat{\mathbf{s}}_{\text{fault}} = \mathbf{B}^T \mathbf{z}_{\text{fault}} \tag{3.4}$$

where $\mathbf{z}_{\text{fault}}$ is the scaled FOC dataset. Then, the monitoring statistic for the sample t under FOC is calculated by Equation 3.5:

$$I_{\text{fault}}^2(t) = \hat{\mathbf{s}}_{\text{fault}}^T(t)\hat{\mathbf{s}}_{\text{fault}}(t) \tag{3.5}$$

After developing the NOC ($\mathbf{x}_{\text{normal}}$) and FOC ($\mathbf{x}_{\text{fault}}$) datasets separately, both ($\mathbf{x}_{\text{normal}}$), ($\mathbf{x}_{\text{fault}}$), the monitoring statistics I^2_{normal} and I^2_{fault} are combined into $\mathbf{x}_{\text{train}}$ and I^2_{train}, respectively.

These combined datasets are then used as input variables in the ICA-SVM algorithm, along with the label vector. Values in the datasets are labeled with +1 for NOC and -1 for FOC. In the second stage, we test the trained ICA-SVM model using newly generated test data, which is scaled in the same manner as the training data. The ICs ($\hat{\mathbf{s}}_{\text{new}}$) are calculated based on this scaled dataset.

$$\hat{\mathbf{s}}_{\text{new}} = \mathbf{B}^T \mathbf{z}_{\text{new}} \tag{3.6}$$

Subsequently, we calculate the monitoring statistics for each sample as outlined below.

$$I^2_{\text{new}}(t) = \hat{\mathbf{s}}^T_{\text{new}}(t)\hat{\mathbf{s}}_{\text{new}}(t) \tag{3.7}$$

The observations are separated using the function

$$f(\mathbf{X}_{\text{test}}) = \operatorname{sgn}\left(\sum_{i=1} \alpha_i y_i K(\mathbf{X}_{\text{train},i}\mathbf{X}_{\text{test}}) + b^*\right) \mathbf{X}_{\text{test}} \in \begin{cases} +1 & \text{if} \quad f(\mathbf{X}_{\text{test}}) > 0 \\ -1 & \text{if} \quad f(\mathbf{X}_{\text{test}}) < 0 \end{cases} \tag{3.8}$$

where $\mathbf{X}_{\text{test}} = \left[\mathbf{x}_{\text{test}}, I^2_{\text{test}}, \mathbf{y}_{\text{test}}\right]$ represents the input vector for the test stage. If $\mathbf{X}_{\text{test}} \in +1$, then it is interpreted as the process running under NOC, whereas $\mathbf{X}_{\text{test}} \in -1$ refers to the process under FOC, we obtained control charts using the proposed hybrid ICA-SVM method. Like all other control charts, the I^2-PoC control chart requires two essential components: the monitoring statistic and the control limit.

The monitoring statistics represent the SVM's estimation of the probability that the observation is out of control. Equation 2.8 is employed to calculate the PoC for the SVM model. Since the distribution of monitoring statistics is unknown, we utilize a non-parametric bootstrap method to establish the control limit. This control limit is determined as the value corresponding to the 99th percentile of the means of I^2-PoC obtained from in-control samples via bootstrapping. If the calculated statistic I^2-PoC exceeds this control limit, it indicates that the process is considered out of control. In the event of any detected shift in the process, an investigation is initiated to identify the sources of this shift.

To detect the shift in the process mean, we use the averages of the SVM output PoC values for out-of-control conditions $\text{POC}_{\{-1\}}$. We compare the means for different shift scenarios and determine the source of the shift based on the largest mean. The flowchart of the multivariate process monitoring procedure is given in Figure 1.

4. Performance evaluation of I^2- PoC control chart: A simulation study

A simulation study was conducted to evaluate the performance of the I^2-PoC control chart for both multivariate normal and non-normal processes. In both scenarios, we considered seven different shift magnitudes. These simulations were carried out on processes involving three variables. The shifts in the process were achieved by modifying specific variables that affected the signal, resulting in various possible combinations. To distinguish between these seven scenarios, we used a numbered notation system. Here, '0' indicated that the process was in control (meaning no shifts in the variables), while '1' indicated that the process was out of control (indicating variable shifts). For example, $(1, 0, 0)$ would mean that only the mean of the first variable had shifted, while the second and third variables remained unchanged.

In this study, for each shift combination, we generated a dataset consisting of 700 in control observations and 300 out-of-control observations. Each individual sample had a specific size 1, (n). Consequently, the simulation study required datasets of 7000 observations for each of training and testing phases, considering the various possible shift combinations $2^{p-1} = 7$ and $p = 3$.

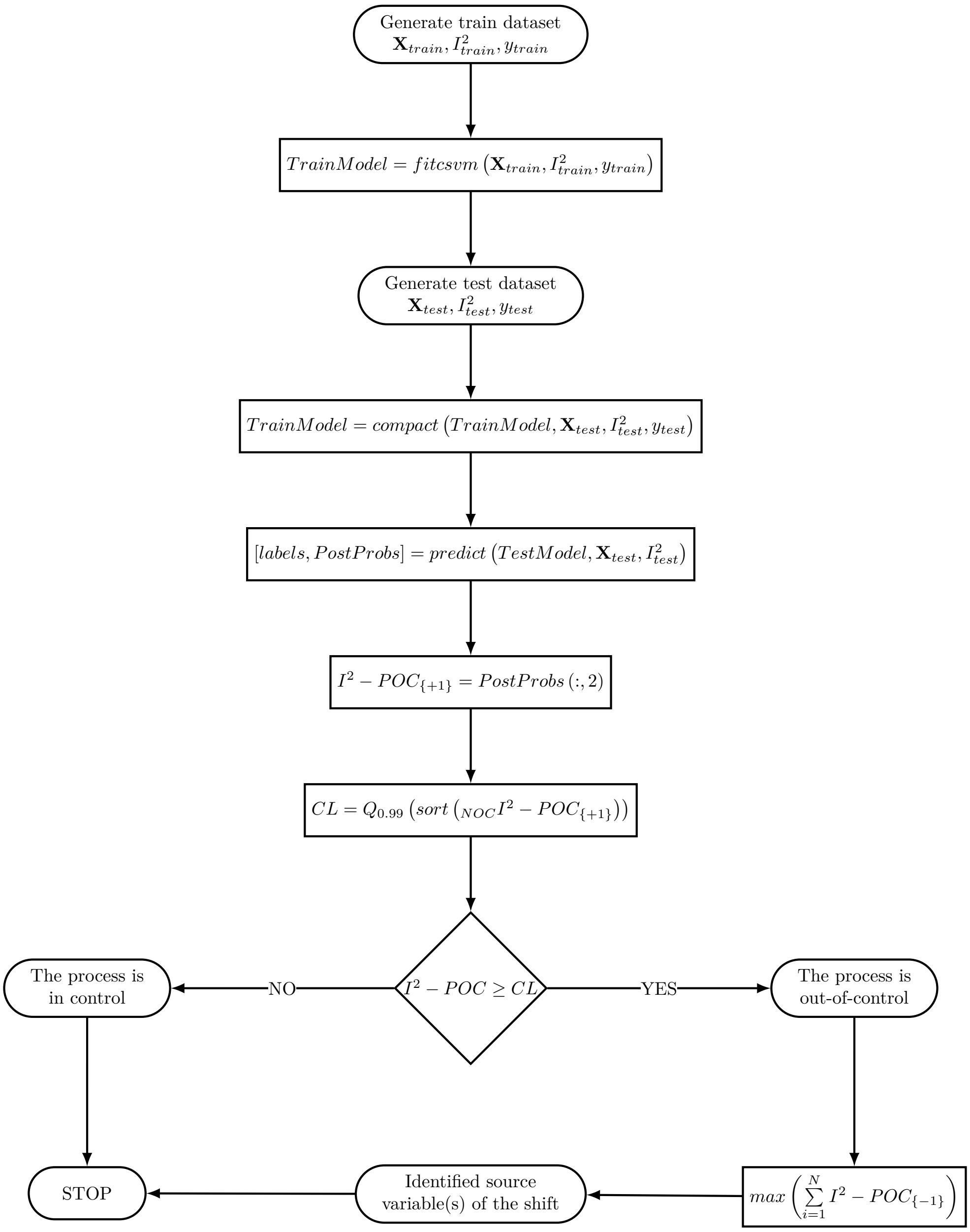

Figure 1. The flowchart of the hybrid ICA-SVM method

The shifts in the target means of the multivariate normal process were performed as $\mu_0 + \delta\sigma_0$. We assumed that the variances of the variables were equal and set to 1. Additionally, we considered three different levels of correlation coefficients between variables: low ($\rho_1 = 0.3$), medium ($\rho_2 = 0.5$), and high ($\rho_3 = 0.8$).

Data for the marginal distribution of multivariate non-normal processes is generated using the gamma distribution with the t-Copula method, $X_i \sim \text{Gamma}\left(\theta_1, \theta_2\right), \quad i = 1, 2, 3$. The parameters θ_1 and θ_2 represent the shape and scale of the gamma distribution, respectively. The skewness coefficient of the gamma distribution $\left(\frac{2}{\sqrt{\theta_1}}\right)$ depends on θ_1. Consequently, as θ_1 increases, the distribution approaches a normal distribution. Since the gamma distribution is defined in the range of $[0, \infty]$, and for the sake of computational convenience, we have chosen both θ_1 and θ_2 to be 0.5 for the in-control process, $(\theta_1 = 0.5, \theta_2 = 0.5)$.

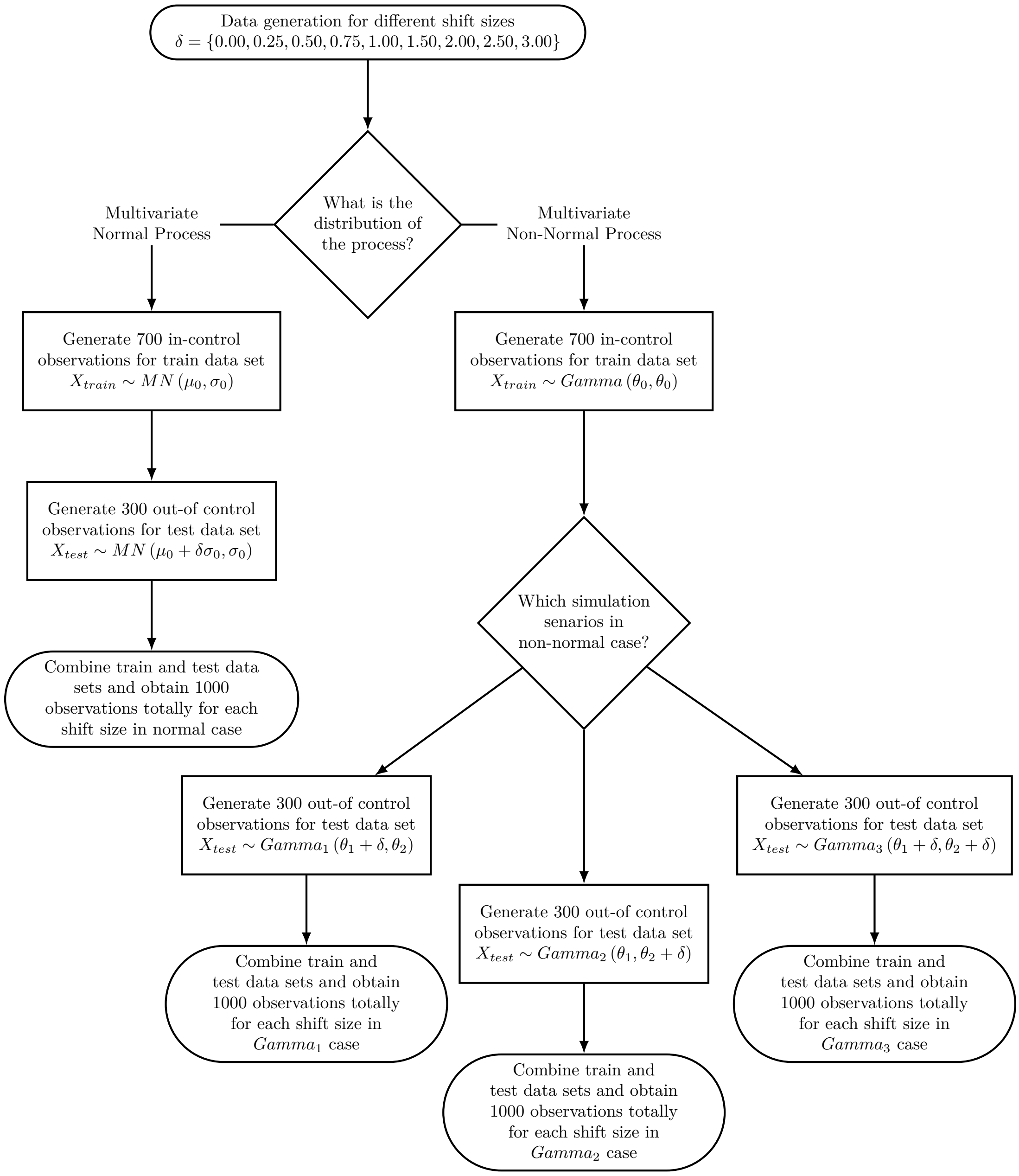

Figure 2. The flowchart of the simulation design

To generate non-normal data, we defined three different simulation scenarios based on the amount of shifts in the gamma distribution parameters (Gamma_1, Gamma_2, Gamma_3). In the first scenario, only θ_1 is shifted, $(\theta_1 + \delta)$. In the second scenario, only θ_2 is shifted, $(\theta_2 + \delta)$ in the third scenario, both θ_1 and θ_2 parameters are shifted, $(\theta_1 + \delta, \theta_2 + \delta)$. The flowchart visualizing the main steps of the simulation procedure is given in Figure 2. The performance of the proposed method is evaluated using the concept of average run length (ARL). ARL represents the average number of samples between two shifts in the process. In a control chart, there are two types of signals: false signals occur when a sample falls outside the control limit even though the process is in control, while correct signals occur when the process is genuinely out of control.

As a result, ARL is calculated differently for these two signal types: and (ARL_1). For false signals, it is calculated as (ARL_0), and for correct signals (ARL_1). In the context of hypothesis testing, the probability of receiving a false signal corresponds to Type I error (α), while the probability of receiving a correct signal corresponds to the power $(1-\beta)$. These probabilities are calculated as the inverses of ARL values: $ARL_0 = 1/\alpha$ and for Type I error and $ARL_1 = 1/1-\beta$ for power.

When a process undergoes a shift, the designed control chart is expected to detect it, on average, after ARL_1 the sample is taken. For a control chart to perform well, it's anticipated that the ARL_0 is high while the ARL_1 is small. Achieving both of these conditions simultaneously is challenging. To assess the control chart's performance, the ARL_0 is set to a fixed value, and the corresponding ARL_1 value is reported. A smaller ARL_1 at a specific value of ARL_0 indicates a better-performing control chart, enabling it to detect process shifts earlier and manage the process with minimal delay.

The performance of the proposed I^2-PoC control chart for the multivariate normal process was compared to that of the multivariate Shewhart control charts (Hotelling's T^2, MCUSUM, and MEWMA control charts), I^2 the control chart, and the PoC control chart. Since the multivariate Shewhart control charts require the assumption of normality, the performance of the I^2-PoC control chart for the multivariate non-normal process was evaluated using only the I^2 and the PoC control charts.

The performance of Hotelling's T^2, MCUSUM, and MEWMA control charts in ARL depends solely on the underlying mean vector and covariance matrix, which are represented through the non-centrality parameter [32]. Hotelling's T^2 control chart calculates control limits using either process sample estimates or known parameters, relying on asymptotic distributions. Meanwhile, for MCUSUM and MEWMA charts, achieving a fixed value for ARL_0 entails defining the "k-factor" in MCUSUM and MEWMA [41].

In the context of the MCUSUM chart, Crosier [9] suggests selecting $k = d/2$ to detect a shift with a magnitude d corresponding to the non-centrality parameter. As for the MEWMA chart, Lowry and Montgomery [31] illustrate optimal schemes for choosing the weighting factor λ, which generally falls between 0.05 and 0.25 . In this study, control limits for MCUSUM and MEWMA control charts were obtained from [41]. Moraes et al. [41] found that a specific value of λ is preferable for the MEWMA chart because it outperforms the MCUSUM chart when $k = 0.5$ corresponds to a target shift detection of a non-centrality value $d = 1$.

Once the k and λ values are set, the control limits h are estimated for the control charts to achieve the same average run length $ARL_0 = 100$. This standardization allows for the results to be compared with other studies.

To assess the effectiveness of the I^2-PoC control chart in identifying the source of a shift, we utilized the average probabilities associated with out-of-control observations. Initially, we computed a reference value using the average probability of receiving false signals (ARL_0) derived from posterior probabilities. Subsequently, we determined the average probabilities of correctly identifying signals (ARL_1) from the posterior probabilities calculated for various shift scenarios. By identifying the combination for ARL_1 in which differs from ARL_0, we can pinpoint the variable(s) responsible for the shift.

All calculations were performed using MATLAB. We conducted 10,000 simulations to assess the effectiveness of SVM-PoC in detecting shifts in the process. Additionally, we conducted 2,000 simulations to evaluate the performance for identification the source of the signal for the proposed control chart.

5. Findings

The findings from the simulation study are presented in the tables. It's important to note that the parameter ARL_0 was consistently set to 100 and $\alpha = 0.01$ for all simulations.

5.1. Findings for the normal case

Table 1 displays the values of ARL_1 for the control charts I^2 - PoC used in the multivariate normal process. The ARL_1 values were calculated at $\rho = 0.3, 0.5$, and 0.8 to demonstrate the impact of correlation between variables on performance. The control chart I^2 - PoC performs exceptionally well for shift sizes of $\delta = 0.25$ or greater. For instance, even when $\delta = 0.25$, the control chart I^2- PoC effectively detects process shifts in the first sample for all correlation values. It is worth noting that the control chart I^2 - PoC performs well for all shift sizes in multivariate normal processes. The degree of correlation between variables does not significantly affect the performance of this proposed method. In fact, the control chart $I^2 -$ PoC successfully detects process shifts, even when dealing with highly correlated data.

Table 1. ARL_1 values of the $I^2 -$ PoC control chart for the multivariate normal process ($ARL_0 = 100$)

Multivariate Normal Distribution ($\boldsymbol{\mu}_0 + \delta\sigma, \boldsymbol{\Sigma}_0$)			
$\boldsymbol{\delta\sigma}$	$\boldsymbol{\rho_1 = 0.3}$	$\boldsymbol{\rho_2 = 0.5}$	$\boldsymbol{\rho_3 = 0.8}$
0.00	98.97	98.67	98.95
0.25	1.19	1.18	1.13
0.50	1.18	1.16	1.12
0.75	1.16	1.14	1.11
1.00	1.13	1.12	1.09
1.50	1.07	1.07	1.06
2.00	1.03	1.03	1.03
2.50	1.01	1.01	1.01
3.00	1.00	1.00	1.00

Table 2 presents the simulation findings related to identifying the source of shifts in the process. In this context, we determine the source variable or variables responsible for the process shift by analyzing various combinations.

The values listed in the "source combination" columns of Table 2 represent the highest mean values, which serve as indicators for identifying the variable or variables responsible for the shift. The hybrid ICA-SVM approach accurately identifies the source variable(s) for all amount of shift in the multivariate normal process. For instance, if we consider $\delta = 1.0$ and $\rho_2 = 0.5$, the highest value recorded is 6.006, corresponding to the combination $(0, 1, 1)$ in the respective column. Therefore, the source variables causing the shift are $\mathbf{x}_2$ and $\mathbf{x}_3$. Similarly, when we have $\delta = 2.5$ and $\rho_1 = 0.3$, the largest value is 16.698 , matching with the combination $(1, 0, 1)$, which signifies that the source variables responsible for the shift are $\mathbf{x}_1$ and $\mathbf{x}_3$. You can interpret the other values in the table in a similar manner.

Table 3 displays the values of various multivariate control charts, including Hotelling's T^2 MCUSUM, MEWMA, as well as I^2, PoC and $I^2 -$ PoC control charts. Among these, Hotelling's T^2 control chart exhibits superior performance in detecting large shifts compared to MEWMA and MCUSUM. This is primarily due to the memoryless nature of Hotelling's T^2 control chart. Conversely, when it comes to detecting small shifts, the MEWMA and MCUSUM charts outperform Hotelling's T^2 chart. Notably, the I^2- PoC control chart delivers the best overall performance. Furthermore, as the correlation level increases, the performance of the PoC and $I^2 -$ PoC control charts remains unaffected by the degree of correlation. In contrast, there is a decline in the performance of the multivariate Shewhart control and I^2 charts as the correlation level increases.

Table 2. I^2-PoC values for different combinations of sources for the multivariate normal process $ARL_0 = 100$

Multivariate Normal Distribution $(\boldsymbol{\mu}_0 + \delta\sigma, \boldsymbol{\Sigma}_0)$

		$\rho_1 = 0.3$							$\rho_2 = 0.5$							$\rho_3 = 0.8$						
$\delta\sigma$		(1,1,1)	(1,1,0)	(1,0,1)	(1,0,0)	(0,1,1)	(0,1,0)	(0,0,1)	(1,1,1)	(1,1,0)	(1,0,1)	(1,0,0)	(0,1,1)	(0,1,0)	(0,0,1)	(1,1,1)	(1,1,0)	(1,0,1)	(1,0,0)	(0,1,1)	(0,1,0)	(0,0,1)
0	0	3.999	3.999	3.999	3.999	3.999	3.999	3.999	3.999	3.999	3.999	3.999	3.999	3.999	3.999	3.999	3.999	3.999	3.999	3.999	3.999	3.999
0.5	(1,1,1)	4.131	4.067	4.062	4.027	4.062	4.021	4.021	4.079	4.054	4.05	4.022	4.036	4.022	4.013	4.048	4.045	4.036	4.022	4.043	4.03	4.024
	(1,1,0)	4.063	4.114	4.014	4.032	4.014	4.033	4.004	4.041	4.152	4.007	4.042	4.009	4.033	4.009	4.019	4.521	4.002	4.138	4.002	4.123	4.031
	(1,0,1)	4.06	4.014	4.12	4.035	4.015	4.004	4.026	4.048	4.005	4.158	4.045	4.005	4.005	4.052	4.032	4.002	4.537	4.159	4.004	4.032	4.148
	(1,0,0)	4.02	4.037	4.053	4.056	4.004	4.002	4.002	4.017	4.052	4.049	4.108	4.009	4.006	4.005	4.006	4.138	4.167	4.424	4.032	4.006	4.007
	(0,1,1)	4.068	4.014	4.012	4.006	4.127	4.034	4.034	4.044	4.007	4.005	4.015	4.164	4.039	4.044	4.025	4.005	4.003	4.038	4.522	4.13	4.126
	(0,1,0)	4.03	4.049	4.004	4.002	4.039	4.057	4.003	4.021	4.051	4.012	4.003	4.051	4.078	4.004	4.01	4.139	4.03	4.006	4.132	4.432	4.01
	(0,0,1)	4.026	4.004	4.041	4.005	4.053	4.004	4.056	4.019	4.01	4.057	4.004	4.037	4.005	4.094	4.017	4.025	4.131	4.006	4.148	4.01	4.44
1	(1,1,1)	5.551	4.663	4.677	4.172	4.654	4.171	4.216	5.179	4.56	4.546	4.156	4.513	4.187	4.175	4.693	4.492	4.43	4.246	4.411	4.258	4.242
	(1,1,0)	4.761	5.585	4.134	4.326	4.142	4.414	4.002	4.433	5.918	4.062	4.476	4.047	4.44	4.005	4.218	9.234	4.111	5.244	4.096	5.132	4.035
	(1,0,1)	4.757	4.131	5.607	4.376	4.144	4.002	4.385	4.423	4.075	5.992	4.493	4.06	4.006	4.455	4.185	4.101	9.162	5.343	4.108	4.035	5.366
	(1,0,0)	4.249	4.407	4.42	4.742	4.006	4.005	4.002	4.168	4.505	4.509	5.197	4.003	4.003	4.003	4.107	5.343	5.361	8.436	4.061	4.05	4.046
	(0,1,1)	4.778	4.127	4.138	4.003	5.563	4.354	4.367	4.42	4.059	4.062	4.007	6.006	4.464	4.466	4.219	4.12	4.121	4.043	9.241	5.227	5.231
	(0,1,0)	4.242	4.456	4.008	4.004	4.377	4.662	4.003	4.167	4.47	4.002	4.002	4.522	5.163	4.004	4.106	5.259	4.053	4.05	5.249	8.614	4.056
	(0,0,1)	4.255	4.003	4.431	4.006	4.419	4.006	4.651	4.172	4.002	4.529	4.005	4.505	4.003	5.116	4.077	4.045	5.374	4.039	5.315	4.044	8.587
1.5	(1,1,1)	9.699	6.551	6.598	4.651	6.563	4.685	4.75	8.479	5.929	5.89	4.687	5.927	4.632	4.611	7.051	5.541	5.603	5.043	5.594	5.063	5.088
	(1,1,0)	6.555	9.413	4.645	5.345	4.611	5.279	4.044	5.582	10.193	4.468	5.629	4.466	5.592	4.091	4.675	14.94	6.227	8.127	6.38	8.003	5.553
	(1,0,1)	6.59	4.63	9.346	5.341	4.561	4.038	5.287	5.544	4.461	10.171	5.562	4.426	4.09	5.486	4.625	6.142	15.006	7.928	6.17	5.56	8.22
	(1,0,0)	5.013	5.645	5.644	7.005	4.132	4.056	4.054	4.661	5.929	5.726	8.329	4.162	4.081	4.087	4.398	8.324	8.597	14.309	5.863	5.379	5.547
	(0,1,1)	6.586	4.584	4.616	4.051	9.402	5.259	5.272	5.521	4.417	4.427	4.068	10.383	5.562	5.565	4.704	6.002	6.191	5.478	14.974	8.154	8.302
	(0,1,0)	4.958	5.64	4.117	4.052	5.676	6.968	4.052	4.66	5.754	4.17	4.08	5.756	8.284	4.077	4.45	8.36	6.09	5.473	8.63	14.178	5.392
	(0,0,1)	4.898	4.124	5.481	4.047	5.496	4.057	6.769	4.648	4.163	5.789	4.07	5.8	4.072	8.315	4.388	6.208	8.486	5.517	8.533	5.481	14.161
2	(1,1,1)	14.204	9.189	9.395	5.564	9.406	5.52	5.581	12.572	8.3	8.327	5.528	8.544	5.72	5.632	10.555	8.645	8.517	7.742	8.538	7.633	7.512
	(1,1,0)	9.709	13.79	6.08	6.751	5.885	6.821	4.388	7.71	14.589	6.252	7.355	6.144	7.53	4.804	5.649	18.18	12.336	12.942	12.932	12.647	11.631
	(1,0,1)	9.556	6.011	13.641	6.918	6.152	4.374	6.99	7.671	6.363	14.472	7.528	6.459	4.803	7.459	5.56	12.465	18.177	12.869	12.499	11.449	12.889
	(1,0,0)	6.43	7.657	7.517	10.312	4.99	4.342	4.327	6.029	8.095	8.34	12.079	5.548	4.749	4.77	5.434	13.817	13.708	17.649	12.357	11.245	11.336
	(0,1,1)	9.4	6.122	5.945	4.39	13.618	6.968	6.911	7.714	6.389	6.414	4.836	14.556	7.701	7.639	5.594	12.426	12.474	11.475	18.192	12.407	12.91
	(0,1,0)	6.725	7.829	5.019	4.379	7.755	10.474	4.364	6.056	8.307	5.564	4.763	8.319	12.341	4.751	5.656	13.86	12.465	11.545	13.799	17.64	11.561
	(0,0,1)	6.645	5.042	7.688	4.369	7.561	4.355	10.176	5.948	5.606	8.238	4.771	8.241	4.665	12.295	5.693	12.568	14.046	11.667	14.011	11.751	17.654
2.5	(1,1,1)	17.014	12.317	12.074	6.831	12.138	6.535	6.992	15.637	11.78	11.956	7.641	11.719	7.459	7.911	13.973	13.077	13.074	11.828	13.014	11.928	11.645
	(1,1,0)	12.988	16.708	9.573	8.889	9.549	8.952	5.853	10.503	17.238	10.388	10.143	10.307	10.207	7.594	7.12	19.488	16.91	16.656	16.979	16.594	16.229
	(1,0,1)	13.002	9.543	16.698	9.066	9.668	5.917	8.697	10.581	10.395	17.368	10.19	10.495	7.473	10.072	7.249	17.005	19.475	16.922	16.943	16.472	16.639
	(1,0,0)	10.049	10.898	10.876	13.634	8.099	5.7	5.538	8.993	11.919	11.936	15.434	10.07	7.526	7.713	8.267	17.669	17.545	19.264	17.083	16.503	16.474
	(0,1,1)	13.202	9.44	9.431	5.865	16.762	8.786	8.996	10.377	9.975	10.294	7.378	17.363	10.066	9.848	6.806	17.027	16.879	16.17	19.49	16.576	16.568
	(0,1,0)	10.021	10.773	8.302	5.644	10.946	13.676	5.653	9.34	11.851	9.909	7.544	11.961	15.473	7.49	8.236	17.629	16.932	16.254	17.639	19.244	16.286
	(0,0,1)	10.145	8.506	11.148	5.766	11.039	5.712	13.587	9.115	9.586	11.962	7.426	11.94	7.573	15.467	8.111	16.837	17.647	16.478	17.616	16.379	19.244
3	(1,1,1)	18.659	14.998	15.31	8.808	15.156	8.417	8.609	17.714	14.525	14.511	9.97	14.515	9.842	9.962	16.421	15.88	15.955	15.288	15.977	15.466	15.291
	(1,1,0)	15.97	18.386	13.123	10.629	13.153	11.044	8.504	13.495	18.841	14.134	12.713	14.397	12.662	11.441	9.778	19.89	19.043	18.855	19.206	18.791	18.815
	(1,0,1)	15.874	13.253	18.438	11.134	13.324	8.802	11.002	13.168	14.289	18.837	12.408	13.985	11.195	12.526	9.576	19.149	19.879	18.94	19.102	18.914	18.866
	(1,0,0)	13.899	14.456	14.351	16.284	12.501	8.77	8.658	13.117	15.459	15.651	17.582	14.276	11.515	11.59	11.171	19.316	19.372	19.793	19.02	18.781	18.716
	(0,1,1)	15.971	13.314	13.373	8.951	18.405	11.008	11.034	13.27	14.502	14.319	11.516	18.806	12.72	12.858	9.623	19.154	19.114	18.929	19.885	18.868	18.71
	(0,1,0)	13.736	14.118	12.704	8.9	14.379	16.206	8.983	13.147	15.64	14.365	11.997	15.614	17.533	11.715	11.108	19.27	19.027	18.7	19.317	19.801	18.728
	(0,0,1)	13.948	12.559	14.303	8.749	14.269	9.049	16.156	12.97	14.269	15.769	11.727	15.738	11.641	17.647	11.138	19.041	19.311	18.799	19.304	18.88	19.782

5.2. Findings for the non-normal case

In Table 4, we present the findings for ARL_1 of I^2- PoC control charts applied to three scenarios (Gamma_1, Gamma_2, Gamma_3) involving multivariate gamma processes. The I^2-PoC control chart consistently performs best when subjected to small shift sizes across all scenarios. Specifically, its performance is most notable when a shift occurs in both parameters θ_1 and θ_2. However, as the correlation value increases, the control chart's performance comparatively deteriorates, particularly when dealing with small shift sizes.

Table 5 presents I^2- PoC values that have been calculated based on the Gamma_1 scenario. The average value of I^2-PoC for scenario Gamma_1 is 2 . The I^2-PoC control chart effectively identifies the source variable(s) responsible for the shift $\delta = 0.50$ for all correlation levels. For instance, we anticipate that the source variables are $\mathbf{x}_2$ and $\mathbf{x}_3$. in the combination $(0, 1, 1)$. Notably, when $\delta = 1.50$ and $\rho_1 = 0.3$ are both present, the highest value in the $(0, 1, 1)$ column (5.087) corresponds to the same combination in the row. This alignment between the same combination in both the row and column indicates the correct identification of the source variable(s). Interestingly, the correlation level does not influence the determination of the source of the shift. The calculated values for the Gamma_2 and Gamma_3 scenarios can be found in supplementary materials Table 7 and Table 8, respectively. The results for scenarios Gamma_2 and Gamma_3 are similar to those of the Gamma_1 scenario.

Table 6 presents ARL_1 values for control charts I^2, PoC and I^2-PoC at various levels of δ and ρ for three different scenarios: Gamma_1, Gamma_2, and Gamma_3. For the Gamma_1 process, the control chart I^2 can only detect a process shift when $\delta = 1.50$ or exceeds 1.50. In contrast, both PoC and I^2-PoC control charts can detect shifts for $\delta = 0.25$. Notably, the PoC control chart outperforms the others when at $\delta = 0.75$ and

Table 3. ARL_1 values of the T^2, MCUSUM, MEWMA, I^2, PoC, and I^2-PoC control charts for the multivariate normal process ($ARL_0 = 100$)

Multivariate Normal Distribution $(\boldsymbol{\mu}_0 + \delta\sigma, \boldsymbol{\Sigma}_0)$						
			$\rho_1 = \mathbf{0.3}$			
$\delta\sigma$	T^2	MCUSUM	MEWMA	I^2	PoC	I^2-PoC
0	99.46	99.44	99.7	99.92	98.48	98.97
0.25	82.27	42.63	38.68	45.45	5.47	1.19
0.5	52.26	15.13	15.72	35.41	4.22	1.18
0.75	28.86	9.65	9.27	14.08	3.81	1.16
1	16.3	6.65	6.59	9.52	3.28	1.13
1.5	5.69	4.1	4.24	3.5	2.04	1.07
2	2.62	3.09	3.18	1.85	1.26	1.03
2.5	1.57	2.44	2.58	1.28	1.06	1.01
3	1.18	2.15	2.19	1.08	1.01	1
			$\rho_2 = \mathbf{0.5}$			
$\delta\sigma$	T^2	MCUSUM	MEWMA	I^2	PoC	I^2-PoC
0	100.14	99.46	100.92	98.57	97.85	98.67
0.25	86.25	48.49	44.15	81.17	5.57	1.18
0.5	58.93	20.49	18.44	39.27	5.35	1.16
0.75	34.93	10.32	10.7	21.74	4.43	1.14
1	20.48	7.41	7.54	11.46	3.97	1.12
1.5	7.7	4.43	4.77	4.4	2.41	1.07
2	3.43	3.46	3.54	2.24	1.55	1.03
2.5	1.97	2.86	2.86	1.47	1.15	1.01
3	1.38	2.34	2.41	1.17	1.03	1
			$\rho_3 = \mathbf{0.8}$			
$\delta\sigma$	T^2	MCUSUM	MEWMA	I^2	PoC	I^2-PoC
0	100.78	100.54	100.87	101.1	97.77	98.95
0.25	89.76	52.43	50.23	84.89	5.88	1.13
0.5	64.05	21.69	21.41	46.42	5.59	1.12
0.75	42.14	12.34	12.8	26.26	4.71	1.11
1	27.05	8.79	8.84	15.1	4.25	1.09
1.5	10.76	5.22	5.46	6	2.91	1.06
2	5.03	3.9	4.04	3	1.79	1.03
2.5	2.74	3.11	3.26	1.85	1.34	1.01
3	1.78	2.81	2.73	1.35	1.1	1

dealing with smaller shifts, regardless of correlation levels. For instance, with $\delta = 0.75$, the average run length (ARL_1) of the I^2 control chart is 11.68 , while the ARL_1 of the I^2-PoC control chart is 1.50 , and the ARL_1 of the PoC control chart is 1.22 . In essence, the PoC control chart can identify minor shifts in the process shape parameter earlier than the other methods. However, for larger shifts ($\delta \geq 0.75$), both the PoC and I^2-PoC control charts perform similarly and better than the I^2 control chart. The performance of the I^2 and PoC control charts tends to deteriorate with increasing correlation, but the I^2-PoC control chart remains unaffected by correlation levels. Notably, the I^2-PoC control chart works well across all correlation levels when a shift occurs solely in the shape parameter for the Gamma_1 scenario. In the case of the Gamma_2 scenario, the I^2 control chart struggles with shifts smaller than 1.5σ, whereas the PoC and I^2-PoC control charts perform well, even with minor process shifts. The PoC control chart excels at detecting small shifts earlier than the other methods. However, for larger shifts ($\delta \geq 1.5$), both

Table 4. ARL_1 values of the I^2 − PoC control chart for the multivariate gamma process ($ARL_0 = 100$)

	Gamma_1			**Gamma_2**			**Gamma_3**		
δ	$\rho_1 = \mathbf{0.3}$			$\rho_2 = \mathbf{0.5}$			$\rho_3 = \mathbf{0.8}$		
0.00	99.02	99.02	99.14	98.67	99.25	99.73	98.86	99.15	99.58
0.25	3.27	3.32	3.46	2.81	2.87	3.11	1.59	1.66	1.71
0.50	1.75	1.93	1.94	1.93	1.95	2.45	1.23	1.26	1.29
0.75	1.48	1.50	1.52	1.65	1.78	1.81	1.06	1.09	1.11
1.00	1.20	1.21	1.26	1.63	1.65	1.73	1.02	1.03	1.05
1.50	1.08	1.08	1.09	1.38	1.39	1.43	1.00	1.00	1.01
2.00	1.03	1.04	1.05	1.32	1.33	1.35	1.00	1.00	1.00
2.50	1.01	1.01	1.02	1.24	1.27	1.29	1.00	1.00	1.00
3.00	1.00	1.00	1.01	1.19	1.23	1.26	1.00	1.00	1.00

Table 5. I^2− PoC values for different combinations of sources for Gamma_1 ($ARL_0 = 100$)

		Gamma_1																				
		$\rho_1 = \mathbf{0.3}$							$\rho_2 = \mathbf{0.5}$							$\rho_3 = \mathbf{0.8}$						
		(1,1,1)	(1,1,0)	(1,0,1)	(1,0,0)	(0,1,1)	(0,1,0)	(0,0,1)	(1,1,1)	(1,1,0)	(1,0,1)	(1,0,0)	(0,1,1)	(0,1,0)	(0,0,1)	(1,1,1)	(1,1,0)	(1,0,1)	(1,0,0)	(0,1,1)	(0,1,0)	(0,0,1)
0	0	2	2	2	2	2	2	2	2	2	2	2	2	2	2	2	2	2	2	2	2	2
	(1,1,1)	2.468	2.241	2.228	2.057	2.211	2.052	2.066	2.321	2.159	2.18	2.048	2.173	2.047	2.049	2.277	2.158	2.185	2.06	2.173	2.062	2.067
	(1,1,0)	2.265	2.305	2.097	2.058	2.1	2.068	2.01	2.212	2.335	2.063	2.061	2.078	2.073	2.005	2.106	2.892	2.028	2.134	2.033	2.151	2.002
	(1,0,1)	2.32	2.108	2.323	2.084	2.105	2.008	2.092	2.216	2.065	2.329	2.073	2.063	2.003	2.074	2.098	2.032	2.9	2.153	2.04	2.001	2.17
0.5	(1,0,0)	2.146	2.131	2.133	2.145	2.022	2.004	2.009	2.107	2.147	2.139	2.194	2.016	2.004	2.003	2.046	2.179	2.193	2.816	2.005	2.001	2.001
	(0,1,1)	2.264	2.095	2.105	2.011	2.346	2.07	2.077	2.207	2.071	2.071	2.005	2.36	2.078	2.069	2.123	2.041	2.036	2.003	2.851	2.187	2.132
	(0,1,0)	2.127	2.157	2.032	2.011	2.12	2.142	2.01	2.12	2.143	2.021	2.01	2.115	2.192	2.003	2.048	2.192	2.004	2.001	2.152	2.861	2.002
	(0,0,1)	2.148	2.032	2.151	2.009	2.116	2.008	2.127	2.117	2.012	2.137	2.003	2.134	2.004	2.193	2.044	2.003	2.182	2	2.155	2.002	2.856
	(1,1,1)	3.889	2.914	2.918	2.219	2.914	2.232	2.22	3.396	2.707	2.674	2.219	2.711	2.201	2.195	2.971	2.736	2.729	2.321	2.752	2.342	2.363
	(1,1,0)	3.039	3.439	2.409	2.299	2.408	2.334	2.049	2.736	3.507	2.314	2.337	2.302	2.331	2.049	2.543	5.181	2.65	2.7	2.597	2.655	2.279
	(1,0,1)	3.09	2.399	3.442	2.322	2.404	2.045	2.305	2.719	2.309	3.599	2.334	2.288	2.037	2.323	2.538	2.601	5.24	2.579	2.593	2.26	2.701
1	(1,0,0)	2.377	2.365	2.382	2.69	2.109	2.024	2.026	2.304	2.393	2.4	3.001	2.101	2.021	2.019	2.358	2.835	2.911	5.159	2.347	2.156	2.144
	(0,1,1)	2.997	2.394	2.392	2.046	3.399	2.351	2.278	2.685	2.272	2.297	2.044	3.624	2.301	2.35	2.598	2.658	2.615	2.281	5.195	2.713	2.645
	(0,1,0)	2.379	2.413	2.106	2.024	2.365	2.626	2.023	2.249	2.367	2.077	2.016	2.362	3.019	2.011	2.313	2.767	2.34	2.147	2.785	5.114	2.153
	(0,0,1)	2.361	2.099	2.401	2.025	2.403	2.02	2.695	2.262	2.077	2.348	2.015	2.385	2.018	3.038	2.323	2.319	2.853	2.132	2.802	2.164	5.142
	(1,1,1)	5.584	3.766	3.737	2.475	3.81	2.408	2.412	4.734	3.511	3.461	2.419	3.446	2.425	2.386	3.929	3.813	3.841	3.065	3.79	3.067	3.087
	(1,1,0)	4.218	4.926	3.007	2.686	3.096	2.655	2.188	3.72	5.093	2.938	2.655	2.927	2.673	2.233	3.517	7.168	4.271	3.702	4.14	3.705	3.343
	(1,0,1)	4.222	2.983	4.897	2.655	3.041	2.158	2.613	3.655	2.967	5.132	2.638	3.007	2.2	2.727	3.466	4.067	7.252	3.829	4.182	3.407	3.665
1.5	(1,0,0)	2.793	2.792	2.824	3.541	2.307	2.059	2.061	2.603	2.743	2.799	4.19	2.341	2.078	2.085	3.119	4.1	4.201	6.967	3.582	2.964	2.991
	(0,1,1)	4.273	2.98	2.961	2.136	5.087	2.69	2.614	3.501	2.904	2.91	2.189	5.309	2.682	2.714	3.522	4.137	4.117	3.364	7.073	3.731	3.781
	(0,1,0)	2.825	2.836	2.341	2.066	2.852	3.607	2.069	2.665	2.873	2.344	2.069	2.891	4.175	2.076	3.138	4.134	3.554	2.983	4.088	6.825	2.947
	(0,0,1)	2.831	2.361	2.806	2.074	2.81	2.084	3.489	2.672	2.39	2.849	2.083	2.808	2.092	4.152	3.221	3.574	4.265	3.059	4.164	3.001	6.909
	(1,1,1)	7.009	4.636	4.681	2.734	4.704	2.718	2.673	6.105	4.451	4.495	2.78	4.327	2.805	2.81	5.343	4.989	4.831	3.974	4.81	3.946	3.979
	(1,1,0)	5.306	6.304	3.96	2.993	3.995	3.09	2.434	4.816	6.713	3.898	3.175	4.017	3.202	2.616	4.514	8.415	5.755	5.132	5.739	5.038	4.792
	(1,0,1)	5.473	4.015	6.461	3.115	3.937	2.364	3.051	4.76	3.965	6.657	3.13	3.928	2.63	3.056	4.557	5.863	8.249	5.273	5.948	4.898	5.235
2	(1,0,0)	3.605	3.482	3.59	4.657	2.825	2.168	2.21	3.511	3.612	3.611	5.276	3.026	2.303	2.283	4.305	5.684	5.722	8.022	5.236	4.468	4.431
	(0,1,1)	5.586	3.918	3.805	2.345	6.434	3.023	3.029	4.882	4.001	4.006	2.642	6.585	3.11	3.175	4.481	5.944	5.815	4.94	8.298	5.127	5.292
	(0,1,0)	3.533	3.579	2.929	2.185	3.494	4.592	2.175	3.409	3.646	2.999	2.285	3.612	5.397	2.261	4.271	5.812	5.459	4.659	5.791	8.169	4.651
	(0,0,1)	3.523	2.896	3.456	2.208	3.532	2.212	4.503	3.493	3.023	3.663	2.268	3.625	2.281	5.477	4.185	5.279	5.789	4.49	5.796	4.775	8.172
	(1,1,1)	7.986	5.481	5.33	2.866	5.507	2.899	2.963	7.263	4.946	4.921	2.964	5.071	3.026	3.025	6.213	6.154	6.014	5.125	6.022	5.07	5.139
	(1,1,0)	6.691	7.542	5.079	3.381	4.994	3.432	2.75	5.835	7.732	5.034	3.74	5.133	3.6	3.194	5.398	9.108	7.076	6.589	7.145	6.532	6.215
	(1,0,1)	6.506	4.981	7.594	3.397	5.033	2.744	3.391	5.829	4.985	7.814	3.685	5.093	3.229	3.674	5.322	7.12	8.918	6.677	7.078	6.212	6.393
2.5	(1,0,0)	4.55	4.283	4.344	5.507	3.718	2.468	2.453	4.641	4.717	4.719	6.534	3.921	2.77	2.673	5.444	6.954	6.997	8.739	6.761	6.138	6.076
	(0,1,1)	6.645	4.889	4.98	2.74	7.598	3.393	3.473	5.876	5.194	5.136	3.167	7.635	3.712	3.747	5.465	7.123	7.076	6.336	8.962	6.473	6.444
	(0,1,0)	4.532	4.409	3.738	2.387	4.329	5.7	2.434	4.677	4.665	4.117	2.698	4.575	6.546	2.688	5.417	7.059	6.84	6.269	7.021	8.76	6.173
	(0,0,1)	4.69	3.797	4.479	2.419	4.368	2.407	5.663	4.6	4.101	4.717	2.855	4.702	2.732	6.434	5.492	6.822	7.063	6.138	7.081	6.115	8.783
	(1,1,1)	8.684	6.273	6.232	3.3	6.229	3.19	3.159	7.919	6.133	6.174	3.757	6.173	3.718	3.718	7.125	6.718	6.666	5.898	6.727	5.864	5.904
	(1,1,0)	7.408	8.166	6.088	3.912	6.115	4.002	3.397	6.63	8.379	6.017	4.311	6.049	4.266	3.912	6.185	9.375	7.857	7.386	7.929	7.506	7.325
	(1,0,1)	7.41	6.041	8.201	3.946	6.09	3.464	3.941	6.715	5.931	8.511	4.248	5.948	3.771	4.093	6.257	7.933	9.249	7.515	7.989	7.424	7.306
3	(1,0,0)	5.695	5.329	5.356	6.467	4.932	2.921	2.787	5.595	5.571	5.679	7.267	5.306	3.476	3.501	6.239	7.993	7.924	9.259	7.667	7.356	7.301
	(0,1,1)	7.49	5.973	6.025	3.222	8.262	3.909	3.94	6.696	6.081	6.211	3.898	8.436	4.309	4.364	6.046	7.903	8.037	7.373	9.384	7.647	7.618
	(0,1,0)	5.69	5.45	4.745	2.911	5.298	6.468	2.862	5.491	5.483	5.2	3.543	5.653	7.21	3.451	6.336	7.92	7.612	7.088	7.96	9.179	7.222
	(0,0,1)	5.741	4.957	5.472	2.852	5.349	2.859	6.518	5.767	5.299	5.679	3.475	5.659	3.629	7.229	6.249	7.681	7.956	7.311	7.884	7.241	9.182

the PoC and I^2− PoC control charts outperform the I^2 control chart. As correlation levels increase, the performance of all three methods deteriorates. Unlike the situation in the Gamma_1 scenario, where the I^2 − PoC control chart remained unaffected by correlation levels when a shift occurred in the shape parameter, it is negatively impacted in the Gamma_2 scenario when a shift occurs in the scale parameter. Remarkably, the performance of the PoC control chart is superior in the Gamma_2 scenario compared to the Gamma_1 scenario.

The PoC and I^2 − PoC control charts outperform the speed of the traditional control chart in detecting process shifts, even at very small sample sizes, across all correlation levels in the scenario Gamma_3. For instance, with low values $\rho_1 = 0.3$ and $\delta = 0.25$, the traditional control chart detects the shift after approximately nine samples, whereas the PoC and I^2-PoC charts can identify it after just one sample. When a shift occurs in both parameters, the performance of I^2, PoC and I^2- PoC control charts remains consistent, unaffected by the correlation levels at $\delta \geq 1.5$. In the case of the multivariate gamma distribution, all methods demonstrate superior performance when a shift occurs in both the shape and scale parameters, compared to situations where the shift occurs in only one of these parameters.

Table 6. ARL_1 values of the I^2, PoC, and I^2-PoC control charts for Gamma_1, Gamma_2 and Gamma_3 senarios ($ARL_0 = 100$).

	$\rho_1 = 0.3$			$\rho_2 = 0.5$			$\rho_3 = 0.8$		
	I^2	PoC	I^2- PoC	I^2	PoC	I^2- PoC	I^2	PoC	I^2- PoC
Gamma_1									
0	100.67	99.97	99.02	100.4	99.83	99.02	100.4	98.76	99.14
0.25	37.74	1.88	3.32	44.9	2.44	3.46	49.95	5.78	3.27
0.5	18.42	1.36	1.93	24.97	1.46	1.93	25.26	1.68	1.75
0.75	11.68	1.22	1.5	14.6	1.26	1.52	15.95	1.57	1.48
1	7.12	1.1	1.2	9.91	1.12	1.21	10.23	1.25	1.26
1.5	3.52	1.03	1.08	4.72	1.05	1.08	5.21	1.11	1.09
2	2.25	1.01	1.05	2.93	1.03	1.03	3.3	1.1	1.05
2.5	1.64	1	1.01	1.94	1.01	1.01	2.39	1.02	1.02
3	1.34	1	1	1.53	1	1	1.81	1.01	1.01
Gamma_2									
0	101.03	97.56	98.67	100.11	98.77	99.25	100.47	98.77	99.73
0.25	23.03	1.5	2.87	24.07	1.99	2.81	24.96	2.02	3.11
0.5	9.41	1.48	1.93	10.64	1.49	1.95	11.6	1.6	2.45
0.75	6.25	1.42	1.65	7.08	1.45	1.78	8.15	1.54	1.81
1	4.4	1.38	1.63	4.97	1.45	1.65	5.89	1.5	1.73
1.5	2.96	1.32	1.38	3.36	1.33	1.39	4.13	1.35	1.43
2	2.36	1.23	1.32	2.7	1.25	1.33	3.24	1.28	1.35
2.5	2.04	1.15	1.24	2.3	1.17	1.27	2.79	1.24	1.29
3	1.84	1.12	1.19	2.08	1.16	1.23	2.49	1.22	1.26
Gamma_3									
0	100.76	99.07	98.86	101.9	100.13	99.15	99.49	98.96	99.58
0.25	9.29	1.33	1.59	11.41	1.37	1.66	14.18	1.53	1.71
0.5	3.17	1.11	1.23	3.7	1.13	1.26	4.53	1.18	1.29
0.75	1.74	1.02	1.06	1.97	1.02	1.09	2.47	1.05	1.11
1	1.27	1.01	1.02	1.41	1.01	1.03	1.66	1.03	1.05
1.5	1.04	1	1	1.08	1	1	1.18	1	1.01
2	1	1	1	1.01	1	1	1.04	1	1
2.5	1	1	1	1	1	1	1.01	1	1
3	1	1	1	1	1	1	1	1	1

6. Conclusion

In order to enhance efficiency and maintain quality within a multivariate process, it is crucial to provide operators with precise information regarding the process's status. However, the practical implementation of MSPC charts presents a challenge. This challenge revolves around the identification of the quality variable(s) responsible for triggering the out-of-control signal.

The objective of this study is to develop a hybrid method capable of not only detecting shifts but also pinpointing the variable(s) responsible for these shifts in both multivariate normal and non-normal processes with correlated data. To achieve this, we considered two distinct processes, one adhering to a normal distribution and the other to a non-normal distribution. Additionally, we examined the correlation levels among the quality variables within the process, categorizing them into three levels: low, medium, and high.

In the context of a multivariate normal process scenario, the performance of the control chart in detecting a shift in the process mean is superior to that of Hotelling's T^2 chart, MCUSUM, MEWMA, I^2 and PoC control charts. Generally, MCUSUM and MEWMA control charts exhibit similar performance and outperform Hotelling's T^2 chart, particularly when the shift in mean is small. The proposed control chart surpasses Shewhart control charts for shift sizes exceeding 1.5, while the PoC control chart outperforms Shewhart control charts even for smaller shifts. In both small and large shift sizes, the proposed I^2-PoC control chart demonstrates superiority over Shewhart, I^2, and PoC control charts. Furthermore, as the correlation level between variables increases, the performance of all other methods tends to diminish proportionally, while the I^2-PoC control chart remains unaffected. These findings highlight the fact that the I^2-PoC control chart is insensitive to both shift size and correlation level in multivariate normal processes, underlining its superior performance in such scenarios.

For non-normal processes, both the PoC and I^2-PoC control charts outperform the standard control chart, even when confronted with small shifts in each scenario. As correlation levels increase, the relative performance of the | I^2 control chart decreases, whereas the performance of the PoC and the I^2-PoC control charts remains unaffected. The PoC and I^2-PoC control chart are insensitivity to shift size and correlation level, coupled with its strong performance in non-normal processes, represents a significant advantage over the alternatives discussed in the literature.

The hybrid ICA-SVM method offers a solution for detecting shifts in processes that conform to both multivariate normal and non-normal distributions, and it effectively identifies the source variable(s) responsible for these shifts. In various scenarios, including different shift sizes and correlation levels within multivariate normal and non-normal processes, the hybrid ICA-SVM method consistently and accurately determines the source of the shift. Our simulation study demonstrates that the performance of this method remains stable, regardless of the degree of correlation among variables when identifying the source of the shift. Consequently, the hybrid ICA-SVM method presents a flexible alternative for monitoring multivariate processes, alleviating the need for the normality assumption found in traditional MSPC charts and remaining unaffected by correlated variables.

The present study plays a crucial role in the field of MSPC by addressing the detection and identification of shifts in both multivariate normal and non-normal processes. Our proposed method stands out as superior compared to similar studies in the literature. In a prior study by Lee et al. [29], they offered a solution for detecting and identifying shifts, but it comes with a computational challenge. As the number of quality variables increases, applying their method becomes increasingly difficult. Similarly, in studies like Chongfuangprinya et al. [8] and Shao et al. [43], the results of their approaches to identifying shifts remain unclear and involve computational complexities.

Our proposed method remains open to further development. For instance, in a multivariate process, an out-of-control situation may manifest in the process distribution itself as well as in the distribution parameters. The proposed method can also be extended to detect shifts occurring simultaneously in both the mean vector and the variance-covariance matrix.

References

[1] F.B. Alt, *Multivariate Quality Control, Encyclopedia of Statistical Sciences*,Vol.6, N.L. Johnson and S. Kotz, (eds.) Wiley, New York, 1985.

[2] L.K. Chan and G.Y. Li, *A multivariate control chart for detecting linear trends*, Comm. Statist. Simulation Comput. **23**, 997-1012, 1994.

[3] Y.S. Chang and D.S. Bai, *A multivariate T2 control chart for skewed populations using weighted standard deviations*,Qual. Reliab. Eng. Int. **20**, 3146, 2004.

[4] J.M. Charnes, *Tests for special causes with multivariate autocorrelated data*, Comput. Oper. Res. **22**, 443-453, 1995.

[5] M.P.S. Chawla, *PCA and ICA processing methods for removal of artifacts and noise in electrocardiograms: A survey and comparison*, Appl. Soft Comput. **11** (2), 2216-2226, 2011.

[6] L.H. Chiang, E.L. Russell and R.D. Braatz, *Fault Detection and Diagnosis in Industrial Systems*, London, U.K., Springer, 2000.

[7] S.W. Choi, C. Lee, J.M. Lee, J.H. Park and I.B. Lee, *Fault detection and identification of nonlinear processes based on kernel PCA*, Chemometrics Intell. Lab. Syst. **75** (1), 55-67, 2005.

[8] P. Chongfuangprinya, S.B. Kim, S.K. Park and T. Sukchotrat, *Integration of support vector machines and control charts for multivariate process monitoring*, J. Stat. Comput. Simul. **81** (9), 1157-1173, 2011.

[9] R.B. Crosier, *Multivariate generalizations of cumulative sum quality-control schemes*, Technometrics **30** (3), 291-303, 1988.

[10] S.X. Ding, *Data-driven design of monitoring and diagnosis systems for dynamic processes: A review of subspace technique based schemes and some recent results*, J. Process Control **24** (2), 431-449, 2014.

[11] Z. Ge, Z. Song and F. Gao, *Review of recent research on data-based process monitoring*, Ind. Eng. Chem. Res. **52** (10), 3543-3562, 2013.

[12] M. Girolami, *Self-Organising Neural Networks*, London, U.K., Springer, 4775, 1999.

[13] Z.O. Guler and M.A. Bakir, *Detection and identification of mean shift using independent component analysis in multivariate processes*, J. Stat. Comput. Simul. **92** (9), 1920-1940, 2022.

[14] T. Hastie and R. Tibshirani, *Classification by pairwise coupling*, Ann. Stat. **26** (2), 451-471, 1998.

[15] D.M. Hawkins, *Regression adjustment for variables in multivariate quality control*, J. Qual. Technol. **25**, 170-182, 1993.

[16] A.J. Hayter and K.L. Tsui, *Identification and quantification in multivariate quality control problems*, J. Qual. Technol. **26** (3), 197,208, 1994.

[17] H. Hotelling, *Multivariate Quality Control, Techniques of Statistical Analysis*, C. Eisenhart, M. W. Hastay, ve W. A. Wallis, eds., New York: McGraw-Hill, 1947.

[18] C.C. Hsu, M.C. Chen and L.S. Chen, *Integrating independent component analysis and support vector machine for multivariate process monitoring*, Comput. Ind. Eng. **59** (1), 146-156, 2010.

[19] C.C. Hsu, L.S. Chen and C.H. Liu, *A process monitoring scheme based on independent component analysis and adjusted outliers*, Int. J. Prod. Res. **48** (6), 1727-1743, 2010.

[20] A. Hyvärinen and E. Oja, *Independent component analysis: algorithms and applications*, Neural Networks **13**, 411-430, 2000.

[21] Q. Jiang, X. Yan and B. Huang, *Performance-driven distributed PCA process monitoring based on fault-relevant variable selection and Bayesian inference*, IEEE Trans. Ind. Electron. **63** (1), 377-386, 2016.

[22] C. Jutten and J. Herault, *Blind separation of sources, part I: An adaptive algorithm based on neuromimetic architecture*, Signal Processing **24** (1), 1991.

[23] M. Kano, S. Tanaka, S. Hasebe, I. Hashimoto and H. Ohno, *Monitoring independent components for fault detection*, Am. J. Chem. Eng. **49** (4), 969-976, 2003.

[24] V. Kecman, *Learning and Soft Computing: Support Vector Machines, Neural Networks, and Fuzzy Logic Models*, Massachusetts Institute of Technology Press, Cambridge, Massachusetts, 2001.

[25] J.V. Kresta, J.F. MacGregor and T.E. Marlin, *Multivariate statistical monitoring of process operating performance*, Can. J. Chem. Eng. **69** (1), 35-47, 1991.

[26] J.M. Lee, K.Y. Chang and I.B. Lee, *Statistical monitoring of dynamic processes based on dynamic independent component analysis*, Chem. Eng. Sci. **59** (14), 2995-3006, 2004.

[27] J.M. Lee, S.J. Qin and I.B. Lee, *Fault detection and diagnosis based on modified independent component analysis*, Am. J. Chem. Eng. **52** (10), 3501-3514, 2006.

[28] J.M. Lee, C.K. Yoo and I.B. Lee, *Fault detection of batch processes using multiway kernel principal component analysis*, Comput. Chem. Eng. **28** (9), 1837-1847, 2004.

[29] J.M. Lee, C.K. Yoo and I.B. Lee, *Statistical process monitoring with independent component analysis*, J. Process Control **14**, 467-485, 2004.

[30] R.Y. Liu, *Control charts for multivariate processes*, J. Am. Stat. Assoc. **90**, 1380-1387, 1995.

[31] C.A. Lowry and D.C. Montgomery, *A review of multivariate control charts*, IIE Transactions **27** (6), 800-810, 1995.

[32] C.A. Lowry, W.H. Woodall, C.W. Champ and S.E. Rigdon, *A multivariate exponentially weighted moving average control chart*, Technometrics **34** (1), 46-53, 1992.

[33] C.J. Lu, *Integrating independent component analysis-based denoising scheme with neural network for stock price prediction*, Expert Syst Appl 37 (10), 7056-7064, 2010.

[34] C.J. Lu, T.S. Lee and C.C. Chiu, *Financial time series forecasting using independent component analysis and support vector regression*, Decis. Support Syst. **47** (2), 115-125, 2009.

[35] C.J. Lu and D.M. Tsai, *Independent component analysis-based defect detection in patterned liquid crystal display surfaces*,Image Vis **2**6 (7), 955-970, 2008.

[36] C.J. Lu, C.M. Wu, C.J. Keng and C.C. Chiu, *Integrated application of SPC/EPC/ICA and neural networks*, Int. J. Prod. Res. **46** (4), 873-893, 2006.

[37] E. Martin, A. Morris and J. Zhang, *Process performance monitoring using multivariate statistical process control* in Control Theory and Applications, IEE Proceedings, 132-144, 1996.

[38] R.L. Mason, C.W. Champ, N.D. Tracy, R.J. Wierda and J.C. Young, *Assessment of multivariate process control techniques*, J. Qual. Technol. **29**, 140-143, 1997.

[39] R.L. Mason, N.D. Tracy and J.C. Young, *Decomposition of T2 for multivariate control chart interpretation*, J. Qual. Technol. **27** (2), 109-119, 1995.

[40] R.L. Mason and J.C. Young, *Multivariate Statistical Process Control With Industrial Application*, Philadelphia: SIAM, 2002.

[41] D.A.O. Moraes, F.L.P. Oliveira and L.H. Duczmal, *On the Hotellings T, MCUSUM and MEWMA control charts performance with different variability sources: A simulation study*,Braz. J. Oper. Prod. Manag. **12**, 196-212, 2015.

[42] J. Platt, *Probabilistic outputs for support vector machines and comparison to regularized likelihood methods*, Advances in Large Margin Classifiers, A. Smola, P. Bartlett, B. Scholkopf, and D. Schuurmans, eds., Cambridge, MA, 6174, 2000.

[43] E.Y. Shao, C.J. Lu and Y.C. Wang, *A Hybrid ICA-SVM approach for determining the quality variables at fault in a multivariate process*, Math. Probl. Eng. **18** (1), 1-12, 2012.

[44] J. Shawe-Taylor and N. Cristianini, *An Introduction to Support Vector Machines and Other Kernel-Based Learning Methods*, Cambridge University Press, New York, 2000.

[45] J.H. Sullivan, Z.G. Stoumbos, R.L. Mason and J.C. Young, *Step-Down analysis for changes in the covariance matrix and other parameters*, J. Qual. Technol. **39**, 66-84, 2007.

[46] R. Sun and F. Tsung, *A Kernel-distance-based multivariate control chart using support vector methods*, Int. J. Prod. Res. **41** (13), 2975-2989, 2003.

[47] V.N. Vapnik, *The Nature of Statistical Learning Theory*, New York: Springer-Verlag, 1995.

[48] V.N. Vapnik and A.J. Chervonenkis, *On the uniform convergence of relative frequencies of events to their probabilities*, Academy of Sciences of the United Soviet Socialist Republic **4**, 181, 1968.

[49] W.H. Woodall, D.J. Spitzner, D.C. Montgomery and S. Gupta, *Using control charts to monitor process and product quality profiles*, J. Qual. Technol. **36**, 309-320, 2004.

[50] C.K. Yoo, J.M. Lee, P.A. Vanrolleghem and I.B. Lee, *On-line monitoring of batch processes using multiway independent component analysis*, Chemom. Intell. Lab. Syst. **71** (2), 151-163, 2004.

[51] Y. Zhang and Y. Zhang, *Fault detection of non-Gaussian processes based on modified independent component analysis*, Chem. Eng. Sci. **65** (16), 4630-4639, 2010.

Appendix A. Supplementary Materials

Table 7. I^2- PoC values for different combinations of sources for Gamma_ 2 $(ARL_0 = 100)$

		Gamma_2 $(\theta_1;\theta_2+\delta)$																				
		$\rho_1 = \mathbf{0.3}$							$\rho_2 = \mathbf{0.5}$							$\rho_3 = \mathbf{0.8}$						
δ		(1,1,1)	(1,1,0)	(1,0,1)	(1,0,0)	(0,1,1)	(0,1,0)	(0,0,1)	(1,1,1)	(1,1,0)	(1,0,1)	(1,0,0)	(0,1,1)	(0,1,0)	(0,0,1)	(1,1,1)	(1,1,0)	(1,0,1)	(1,0,0)	(0,1,1)	(0,1,0)	(0,0,1)
0	0	3.999	3.999	3.999	3.999	3.999	3.999	3.999	3.999	3.999	3.999	3.999	3.999	3.999	3.999	3.999	3.999	3.999	3.999	3.999	3.999	3.999
	(1,1,1)	4.387	4.192	4.156	4.057	4.182	4.062	4.066	4.269	4.155	4.153	4.046	4.157	4.044	4.062	4.235	4.157	4.146	4.053	4.171	4.058	4.063
	(1,1,0)	4.262	4.195	4.149	4.06	4.138	4.055	4.031	4.219	4.18	4.109	4.06	4.125	4.06	4.016	4.192	4.201	4.083	4.08	4.096	4.084	4.016
	(1,0,1)	4.249	4.127	4.2	4.061	4.123	4.027	4.062	4.23	4.113	4.188	4.057	4.118	4.016	4.064	4.183	4.081	4.209	4.082	4.094	4.015	4.079
0.5	(1,0,0)	4.179	4.114	4.118	4.062	4.077	4.025	4.028	4.15	4.105	4.106	4.077	4.063	4.022	4.021	4.139	4.126	4.138	4.131	4.044	4.013	4.024
	(0,1,1)	4.29	4.143	4.154	4.032	4.195	4.072	4.046	4.216	4.099	4.113	4.028	4.188	4.058	4.059	4.184	4.095	4.113	4.014	4.221	4.086	4.091
	(0,1,0)	4.19	4.105	4.081	4.019	4.105	4.074	4.022	4.167	4.136	4.059	4.021	4.125	4.098	4.016	4.141	4.139	4.037	4.01	4.13	4.152	4.013
	(0,0,1)	4.171	4.071	4.121	4.017	4.1	4.03	4.068	4.162	4.06	4.11	4.021	4.114	4.016	4.07	4.139	4.04	4.139	4.011	4.145	4.016	4.158
	(1,1,1)	5.25	4.624	4.631	4.242	4.72	4.243	4.26	4.995	4.602	4.605	4.247	4.624	4.236	4.247	4.749	4.581	4.615	4.292	4.577	4.289	4.28
	(1,1,0)	4.853	4.773	4.495	4.259	4.46	4.24	4.122	4.807	4.659	4.425	4.256	4.442	4.243	4.091	4.685	4.902	4.441	4.426	4.425	4.44	4.13
	(1,0,1)	4.894	4.486	4.743	4.247	4.478	4.126	4.214	4.743	4.411	4.624	4.236	4.388	4.1	4.254	4.586	4.386	4.782	4.369	4.367	4.095	4.357
1	(1,0,0)	4.553	4.377	4.371	4.276	4.248	4.084	4.071	4.417	4.379	4.36	4.3	4.174	4.061	4.064	4.374	4.475	4.51	4.707	4.16	4.059	4.05
	(0,1,1)	4.988	4.544	4.528	4.124	4.804	4.281	4.261	4.737	4.44	4.393	4.109	4.642	4.226	4.277	4.652	4.399	4.425	4.091	4.833	4.438	4.406
	(0,1,0)	4.509	4.354	4.231	4.086	4.354	4.282	4.081	4.39	4.309	4.175	4.063	4.347	4.253	4.076	4.392	4.52	4.139	4.063	4.454	4.689	4.058
	(0,0,1)	4.496	4.217	4.324	4.07	4.342	4.081	4.271	4.484	4.189	4.408	4.065	4.36	4.074	4.317	4.371	4.137	4.462	4.056	4.463	4.058	4.675
	(1,1,1)	6.384	5.194	5.297	4.458	5.166	4.517	4.524	5.863	5.22	5.198	4.514	5.214	4.494	4.506	5.314	5.15	5.094	4.619	5.124	4.627	4.636
	(1,1,0)	5.733	5.487	5.019	4.518	4.959	4.501	4.281	5.364	5.263	4.79	4.521	4.852	4.529	4.23	5.262	5.674	4.879	4.925	4.913	4.877	4.295
	(1,0,1)	5.683	5.037	5.485	4.509	4.937	4.309	4.513	5.375	4.85	5.241	4.565	4.881	4.238	4.533	5.202	4.906	5.558	4.879	4.885	4.316	4.86
1.5	(1,0,0)	4.854	4.696	4.679	4.581	4.382	4.161	4.155	4.793	4.756	4.694	4.583	4.374	4.148	4.14	4.708	4.835	4.895	5.36	4.357	4.174	4.151
	(0,1,1)	5.647	4.968	4.977	4.285	5.527	4.509	4.467	5.45	4.894	4.845	4.248	5.236	4.534	4.551	5.291	4.963	4.874	4.368	5.738	4.964	4.935
	(0,1,0)	4.884	4.71	4.436	4.147	4.712	4.585	4.156	4.756	4.634	4.359	4.132	4.634	4.563	4.144	4.765	4.954	4.366	4.165	4.949	5.403	4.182
	(0,0,1)	4.931	4.447	4.701	4.16	4.725	4.153	4.556	4.76	4.369	4.608	4.135	4.642	4.13	4.571	4.694	4.338	4.851	4.159	4.844	4.17	5.302
	(1,1,1)	7.217	5.862	5.905	4.831	5.892	4.777	4.73	6.534	5.778	5.74	4.825	5.78	4.885	4.88	6.064	5.535	5.516	4.887	5.597	4.902	4.934
	(1,1,0)	6.503	6.239	5.591	4.821	5.563	4.859	4.499	6.015	5.911	5.297	4.838	5.365	4.818	4.422	5.836	6.357	5.437	5.407	5.45	5.443	4.609
	(1,0,1)	6.53	5.609	6.183	4.856	5.604	4.521	4.834	6.025	5.301	5.852	4.822	5.308	4.415	4.811	5.71	5.696	6.828	5.614	5.679	4.75	5.568
2	(1,0,0)	5.418	5.128	5.106	4.958	4.777	4.247	4.266	5.263	5.027	5.023	4.961	4.569	4.256	4.222	5.17	5.415	5.315	6.115	4.786	4.384	4.392
	(0,1,1)	6.468	5.608	5.594	4.482	6.227	4.838	4.854	5.971	5.371	5.354	4.446	5.926	4.83	4.862	5.9	5.584	5.504	4.707	6.559	5.453	5.419
	(0,1,0)	5.41	5.089	4.729	4.275	5.092	4.901	4.253	5.235	5.049	4.63	4.253	5.056	4.96	4.255	5.203	5.496	4.733	4.393	5.496	6.098	4.378
	(0,0,1)	5.36	4.676	5.033	4.246	4.999	4.258	4.963	5.198	4.639	5.044	4.266	5.012	4.235	4.946	5.188	4.75	5.433	4.37	5.425	4.357	6.061
	(1,1,1)	8.225	6.572	6.48	5.036	6.659	5.101	5.036	7.194	6.287	6.303	5.12	6.363	5.154	5.136	6.754	6.139	6.077	5.365	6.156	5.365	5.269
	(1,1,0)	7.29	6.94	6.191	5.177	6.23	5.169	4.774	6.641	6.406	5.853	5.123	5.858	5.198	4.663	6.317	7.579	6.251	6.18	6.306	6.115	5.195
	(1,0,1)	7.394	6.187	6.89	5.149	6.15	4.755	5.169	6.847	5.976	6.451	5.228	6.021	4.741	5.232	6.583	6.151	7.255	5.989	6.125	5.062	6.007
2.5	(1,0,0)	5.744	5.37	5.332	5.257	5.039	4.37	4.377	5.623	5.384	5.461	5.333	4.859	4.348	4.356	5.528	5.755	5.828	6.689	5.054	4.523	4.512
	(0,1,1)	7.379	6.27	6.259	4.815	6.839	5.208	5.201	6.842	5.937	6.032	4.759	6.512	5.078	5.25	6.563	6.11	6.052	5.063	7.305	5.929	5.948
	(0,1,0)	5.869	5.439	5.058	4.392	5.466	5.256	4.405	5.498	5.3	4.874	4.329	5.242	5.257	4.324	5.741	5.901	5.19	4.632	5.902	6.792	4.62
	(0,0,1)	5.857	4.983	5.457	4.399	5.443	4.384	5.211	5.543	4.922	5.386	4.353	5.333	4.373	5.269	5.767	5.205	5.943	4.637	5.887	4.65	6.894
	(1,1,1)	8.868	7.145	7.132	5.355	7.067	5.383	5.358	7.611	6.766	6.792	5.317	6.776	5.415	5.382	7.499	6.64	6.73	5.749	6.658	5.743	5.72
	(1,1,0)	7.981	7.5	6.727	5.517	6.81	5.566	5.108	7.416	6.892	6.406	5.485	6.498	5.603	5.016	7.045	7.902	6.671	6.5	6.771	6.55	5.516
	(1,0,1)	8.026	6.832	7.553	5.57	6.731	5.084	5.432	7.241	6.347	6.903	5.457	6.357	4.943	5.567	6.923	6.459	7.677	6.361	6.533	5.335	6.291
3	(1,0,0)	6.242	5.764	5.841	5.639	5.366	4.549	4.522	6.017	5.712	5.751	5.535	5.226	4.531	4.507	6.219	6.476	6.499	7.395	5.665	4.899	4.969
	(0,1,1)	8.073	6.805	6.833	5.073	7.448	5.537	5.479	7.44	6.46	6.473	4.978	7.055	5.55	5.58	6.839	7	7.033	5.795	8.485	6.967	6.839
	(0,1,0)	6.16	5.767	5.339	4.545	5.766	5.593	4.543	5.999	5.72	5.128	4.492	5.731	5.635	4.511	6.447	6.797	5.832	5.111	6.608	7.635	5.072
	(0,0,1)	6.204	5.353	5.748	4.534	5.798	4.54	5.636	5.987	5.241	5.664	4.465	5.642	4.496	5.57	6.008	5.445	6.277	4.805	6.224	4.776	7.172

Table 8. I^2- PoC values for different combinations of sources for Gamma_ 3 $(ARL_0 = 100)$

		Gamma_3 $(\theta_1+\delta;\theta_2+\delta)$																				
$\delta\sigma$		$\rho_1 = \mathbf{0.3}$							$\rho_2 = \mathbf{0.5}$							$\rho_3 = \mathbf{0.8}$						
		(1,1,1)	(1,1,0)	(1,0,1)	(1,0,0)	(0,1,1)	(0,1,0)	(0,0,1)	(1,1,1)	(1,1,0)	(1,0,1)	(1,0,0)	(0,1,1)	(0,1,0)	(0,0,1)	(1,1,1)	(1,1,0)	(1,0,1)	(1,0,0)	(0,1,1)	(0,1,0)	(0,0,1)
0	0	2	2	2	2	2	2	2	2	2	2	2	2	2	2	2	2	2	2	2	2	2
	(1,1,1)	4.008	3.362	3.285	2.467	3.311	2.482	2.479	3.603	3.13	3.122	2.463	3.077	2.438	2.455	3.117	3.037	3.02	2.615	3.065	2.563	2.59
	(1,1,0)	3.55	3.402	2.915	2.465	2.92	2.501	2.241	3.195	3.298	2.772	2.507	2.781	2.511	2.224	3.057	4.39	2.943	2.98	2.941	2.917	2.51
	(1,0,1)	3.505	2.871	3.366	2.476	2.956	2.263	2.484	3.114	2.67	3.279	2.479	2.698	2.232	2.408	2.995	2.966	4.352	2.92	2.923	2.511	2.935
0.5	(1,0,0)	2.755	2.606	2.66	2.623	2.382	2.113	2.116	2.563	2.59	2.603	2.812	2.278	2.098	2.095	2.61	2.984	3.002	4.552	2.494	2.27	2.254
	(0,1,1)	3.483	2.934	2.951	2.269	3.393	2.51	2.493	3.22	2.743	2.747	2.25	3.319	2.459	2.458	2.913	2.899	2.904	2.478	4.193	2.924	2.843
	(0,1,0)	2.803	2.691	2.409	2.124	2.684	2.58	2.14	2.606	2.596	2.302	2.092	2.597	2.914	2.096	2.639	2.95	2.491	2.254	2.86	4.457	2.252
	(0,0,1)	2.81	2.391	2.722	2.124	2.692	2.124	2.624	2.555	2.274	2.546	2.104	2.552	2.1	2.792	2.611	2.578	2.983	2.253	2.945	2.258	4.484
	(1,1,1)	7.721	6.681	6.657	4.537	6.678	4.623	4.549	6.901	6.26	6.28	4.669	6.266	4.664	4.666	6.133	6.259	6.361	5.655	6.462	5.751	5.717
	(1,1,0)	7.109	6.805	6.199	4.649	6.215	4.652	4.22	6.488	6.56	5.951	4.715	5.903	4.792	4.413	6.044	7.463	6.527	6	6.451	5.991	5.83
	(1,0,1)	7.041	6.197	6.778	4.671	6.259	4.204	4.597	6.458	5.913	6.629	4.789	5.893	4.384	4.811	5.968	6.412	7.328	5.907	6.411	5.712	6.11
1	(1,0,0)	5.391	4.99	4.956	4.91	4.838	3.446	3.471	5.408	5.119	5.119	5.586	4.919	3.705	3.774	5.677	6.247	6.275	7.646	6.21	5.541	5.505
	(0,1,1)	7.234	6.224	6.213	4.229	6.943	4.664	4.669	6.559	6.036	6.033	4.461	6.784	4.85	4.875	5.972	6.382	6.38	5.87	7.3	5.855	5.899
	(0,1,0)	5.447	5.097	4.912	3.525	5.066	4.997	3.506	5.184	5.053	4.819	3.702	5.112	5.513	3.653	5.755	6.213	6.227	5.56	6.214	7.601	5.669
	(0,0,1)	5.453	4.973	5.11	3.525	5.187	3.544	5.044	5.275	4.806	5.023	3.702	5.071	3.63	5.545	5.82	6.237	6.395	5.665	6.281	5.547	7.757
	(1,1,1)	9.359	8.674	8.674	6.486	8.556	6.673	6.462	8.812	8.356	8.402	6.924	8.387	7.049	6.948	8.127	8.396	8.389	8.054	8.472	8.073	8.022
	(1,1,0)	9.08	8.961	8.51	6.958	8.506	6.974	6.536	8.755	8.882	8.484	7.394	8.389	7.331	7.034	8.049	8.951	8.434	8.342	8.537	8.35	8.172
	(1,0,1)	8.987	8.372	8.898	6.983	8.469	6.465	6.953	8.473	8.136	8.518	7.133	8.258	7.054	7.098	8.047	8.485	8.925	8.198	8.41	8.161	8.244
1.5	(1,0,0)	7.691	7.484	7.548	7.316	7.476	6.065	6.168	7.67	7.549	7.578	7.637	7.432	6.482	6.405	7.726	8.058	8.084	8.786	8	7.711	7.838
	(0,1,1)	9.016	8.528	8.492	6.674	8.9	6.938	6.999	8.711	8.314	8.287	6.896	8.977	7.403	7.347	8.124	8.456	8.523	8.236	8.943	8.256	8.266
	(0,1,0)	7.77	7.522	7.399	6.079	7.528	7.295	6.134	7.497	7.469	7.427	6.295	7.457	7.643	6.287	7.729	8.064	8.02	7.738	8.09	8.775	7.708
	(0,0,1)	7.658	7.405	7.401	5.964	7.461	6.132	7.274	7.649	7.444	7.615	6.475	7.476	6.444	7.699	7.53	7.934	7.906	7.52	7.889	7.576	8.684
	(1,1,1)	9.788	9.438	9.476	8.016	9.463	7.963	8.115	9.623	9.307	9.321	8.26	9.285	8.222	8.16	9.309	9.213	9.186	8.81	9.2	8.783	8.863
	(1,1,0)	9.724	9.722	9.31	8.46	9.356	8.4	7.818	9.401	9.581	9.189	8.654	9.106	8.71	8.304	8.961	9.559	9.156	9.272	9.224	9.274	9.041
	(1,0,1)	9.718	9.41	9.658	8.322	9.38	8.057	8.467	9.516	9.276	9.571	8.737	9.273	8.571	8.706	9.133	9.313	9.52	9.225	9.351	9.185	9.204
2	(1,0,0)	8.978	8.901	8.905	8.658	8.831	7.919	7.97	9.222	9.11	9.14	9.124	9.077	8.422	8.346	8.712	8.978	8.96	9.265	8.955	8.778	8.747
	(0,1,1)	9.728	9.351	9.35	7.963	9.719	8.337	8.337	9.534	9.316	9.319	8.482	9.669	8.646	8.838	9.199	9.457	9.433	9.272	9.66	9.36	9.421
	(0,1,0)	9.16	8.964	8.953	8.024	9.017	8.723	8.021	9.149	9.125	9.046	8.359	9.157	9.155	8.398	9.131	9.341	9.348	9.153	9.335	9.59	9.191
	(0,0,1)	9.307	9.132	9.16	8.117	9.209	8.075	8.919	8.836	8.758	8.73	8.095	8.731	8.142	8.745	8.79	9.056	9.043	8.841	9.057	8.805	9.322
	(1,1,1)	9.952	9.802	9.831	8.799	9.826	8.801	8.847	9.875	9.723	9.734	8.864	9.712	8.86	8.88	9.704	9.583	9.586	9.129	9.587	9.161	9.193
	(1,1,0)	9.945	9.88	9.816	9.233	9.81	9.209	8.593	9.838	9.868	9.677	9.386	9.673	9.437	8.735	9.572	9.91	9.492	9.695	9.504	9.696	8.742
	(1,0,1)	9.934	9.791	9.896	9.246	9.782	8.675	9.14	9.842	9.701	9.87	9.4	9.706	9.063	9.348	9.65	9.564	9.871	9.693	9.618	9.19	9.717
2.5	(1,0,0)	9.742	9.719	9.661	9.513	9.678	9.123	9.109	9.806	9.736	9.745	9.765	9.705	9.308	9.23	9.588	9.649	9.659	9.74	9.642	9.538	9.588
	(0,1,1)	9.93	9.8	9.791	8.656	9.889	9.164	9.236	9.861	9.663	9.695	8.8	9.836	9.295	9.296	9.508	9.397	9.392	8.783	9.789	9.577	9.592
	(0,1,0)	9.719	9.697	9.67	9.052	9.63	9.492	9.08	9.585	9.541	9.5	9.209	9.528	9.493	9.177	9.643	9.754	9.74	9.682	9.745	9.845	9.673
	(0,0,1)	9.74	9.669	9.683	9.102	9.695	9.111	9.525	9.785	9.701	9.689	9.228	9.706	9.287	9.703	9.685	9.731	9.768	9.7	9.799	9.723	9.857
	(1,1,1)	9.988	9.902	9.943	9.459	9.957	9.424	9.452	9.967	9.906	9.932	9.444	9.916	9.396	9.447	9.893	9.806	9.825	9.537	9.828	9.496	9.462
	(1,1,0)	9.985	9.952	9.939	9.575	9.939	9.64	9.416	9.963	9.949	9.925	9.643	9.9	9.624	9.399	9.889	9.948	9.786	9.836	9.784	9.814	9.237
	(1,0,1)	9.973	9.949	9.963	9.616	9.957	9.441	9.617	9.948	9.911	9.952	9.671	9.887	9.358	9.667	9.881	9.819	9.934	9.814	9.807	9.32	9.775
3	(1,0,0)	9.857	9.859	9.869	9.717	9.867	9.5	9.496	9.923	9.868	9.858	9.811	9.855	9.627	9.62	9.822	9.882	9.882	9.924	9.873	9.807	9.823
	(0,1,1)	9.971	9.949	9.947	9.411	9.965	9.635	9.551	9.956	9.891	9.882	9.252	9.943	9.676	9.669	9.885	9.749	9.745	9.161	9.931	9.767	9.783
	(0,1,0)	9.925	9.883	9.864	9.517	9.892	9.746	9.578	9.943	9.899	9.886	9.637	9.902	9.875	9.657	9.891	9.905	9.832	9.706	9.889	9.937	9.68
	(0,0,1)	9.958	9.904	9.914	9.494	9.931	9.537	9.815	9.909	9.845	9.896	9.665	9.895	9.665	9.846	9.848	9.835	9.928	9.758	9.924	9.709	9.945